



Contents lists available at ScienceDirect

Quaternary Science Reviews

journal homepage: www.elsevier.com/locate/quascirev

Holocene climate variability in Texas, USA: An integration of existing paleoclimate data and modeling with a new, high-resolution speleothem record

Corinne I. Wong ^{a,*}, Jay L. Banner ^b, MaryLynn Musgrove ^c^a Dept. of Earth and Environmental Science, Boston College, USA^b Dept. of Geological Sciences, The University of Texas at Austin, USA^c Texas Water Science Center, U.S. Geological Survey, USA

ARTICLE INFO

Article history:

Received 10 January 2015

Received in revised form

17 June 2015

Accepted 19 June 2015

Available online xxx

Keywords:

Speleothem

Holocene

Texas

Paleoclimate reconstruction

ABSTRACT

Delineating the climate processes governing precipitation variability in drought-prone Texas is critical for predicting and mitigating climate change effects, and requires the reconstruction of past climate beyond the instrumental record. We synthesize existing paleoclimate proxy data and climate simulations to provide an overview of climate variability in Texas during the Holocene. Conditions became progressively warmer and drier transitioning from the early to mid Holocene, culminating between 7 and 3 ka (thousand years ago), and were more variable during the late Holocene. The timing and relative magnitude of Holocene climate variability, however, is poorly constrained owing to considerable variability among the different records. To help address this, we present a new speleothem (NBJ) reconstruction from a central Texas cave that comprises the highest resolution proxy record to date, spanning the mid to late Holocene. NBJ trace-element concentrations indicate variable moisture conditions with no clear temporal trend. There is a decoupling between NBJ growth rate, trace-element concentrations, and $\delta^{18}\text{O}$ values, which indicate that (i) the often direct relation between speleothem growth rate and moisture availability is likely complicated by changes in the overlying ecosystem that affect subsurface CO₂ production, and (ii) speleothem $\delta^{18}\text{O}$ variations likely reflect changes in moisture source (i.e., proportion of Pacific-vs. Gulf of Mexico-derived moisture) that appear not to be linked to moisture amount.

© 2015 Elsevier Ltd. All rights reserved.

1. Introduction

Holocene climate (beginning 11.7 ka [thousand years ago]) was anomalously stable relative to the last glaciation and previous glacial-interglacial cycles, and late Holocene climate (4–0 ka) is a close analogue to the modern (20th and 21st century) climate state. Projections of 21st century climate change forecast global temperatures in excess of the warmest Holocene conditions, which is notable when considering that the development of human civilization has occurred entirely within the Holocene (Marcott et al., 2013). A comprehensive understanding of Holocene climate is relevant to predicting and mitigating future climate change effects.

Developing a comprehensive understanding of the nature and drivers of Holocene climate variability requires the reconstruction of past climate, beyond the instrumental record, from climate archives. There are many different types of climate proxies preserved in climate archives, each reflecting a distinct aspect of the climate system in a unique way. Compiling a comprehensive picture of regional climate for a given interval requires careful consideration of similarities and differences of available proxy records and the relative strengths and weaknesses of each proxy.

Delineating controls on climate variability in Texas is important and challenging for several reasons. According to the U.S. Census Bureau, Texas's economy and population are the second largest in the U.S., and both are among the fastest growing in the Nation (USA Today, 2014). Texas is prone to drought, and the 2011 drought, for example, resulted in agricultural damages of \$9 billion (Austin American-Statesman, 2011). Climatic processes governing past, current, and future drought in Texas are poorly understood,

* Corresponding author.

E-mail address: wongcw@bc.edu (C.I. Wong).

however, in part because there is no one specific precipitation regime that dominates the climate. Instead, Texas is characterized by large year-to-year precipitation variability that is influenced by multiple precipitation regimes. These include the winter Pacific westerly storm track (Feng et al., 2014a; Seager et al., 2007), the North American Monsoon and Great Plains Low Level Jet that drive summer moisture patterns in the southwestern and midwestern U.S. (Higgins et al., 1997; Higgins, 1997), and the North Atlantic Subtropical High that influences summer precipitation in the southeastern U.S. (Hu et al., 2011).

High-resolution records of Holocene climate from proxy reconstructions pertaining to Texas are few compared to numerous glacial-deglacial records, including speleothem records (Feng et al., 2014a; Musgrove et al., 2001) and 20th century tree ring and speleothem records (Cleaveland et al., 2011; Feng et al., 2014b). Existing Holocene records from in and near Texas are largely discontinuous, with few age constraints, and for which proxies have a complex, and sometimes ambiguous, relation to the climate system. We present a new high-resolution speleothem (NBJ) reconstruction of mid to late Holocene climate (7–0 ka), and integrate our findings into a synthesis of Holocene paleoclimate proxy data from in and near Texas (including Oklahoma, southeastern New Mexico, and northern Mexico; hereafter, Texas) and existing static and transient paleoclimate model simulations that span the Holocene. We find that the NBJ $\delta^{13}\text{C}$ record corresponds well with the general evolution of Holocene climate indicated by other records from Texas (e.g., Nordt et al., 2002; Cooke et al., 2003; Ellwood and Gose, 2006). Paleoclimate model simulations are consistent with proxy data that indicate a warmer and drier mid (8.2–4 ka) to late Holocene (4–0 ka), relative to the early (11.7–8.2 ka) Holocene, but model results do not simulate late Holocene climate variability preserved in the proxy records. NBJ trace-element concentrations vary independently from $\delta^{18}\text{O}$ values, indicating a possible decoupling between moisture amount and supply. NBJ $\delta^{18}\text{O}$ variability does not correspond well with speleothem and sea surface temperature (SST) records from the broader region (including the Gulf of Mexico and the southwestern U.S.), but $\delta^{18}\text{O}$ variability is similar to a reconstruction of the Atlantic Meridional Overturning Circulation (Thornalley et al., 2009).

2. Controls on present day climate

Texas spans a transition region between sub-humid to semi-arid climates and is prone to drought (Larkin and Bomar, 1983). There is pronounced seasonality in temperatures (Fig. 1). Precipitation amounts are generally larger in spring and fall compared to summer and winter but vary greatly. The interannual variability of precipitation exceeds the intra-annual variability, indicating an absence of well-defined wet/dry seasons (Fig. 1). Spring and summer precipitation is associated with the Great Plains low-level jet that transports Gulf of Mexico (GoM) moisture to the continental U.S. (Higgins et al., 1997). Large precipitation events can occur in summer and early fall in association with tropical storms, which occasionally have an eastern tropical Pacific origin and a trajectory crossing the GoM. Late fall and winter precipitation is often triggered by the arrival of northern cold fronts associated with the Pacific winter storm track that also provides much of the western U.S. with the majority of its annual precipitation (Seager et al., 2007).

Studies of the principle sources of continental precipitation delineate several oceanic moisture sources for Texas. Forward-tracking models find that the GoM and Caribbean and the tropical north Atlantic are year-round moisture sources, though their influence is more pronounced during the summer (Gimeno et al.,

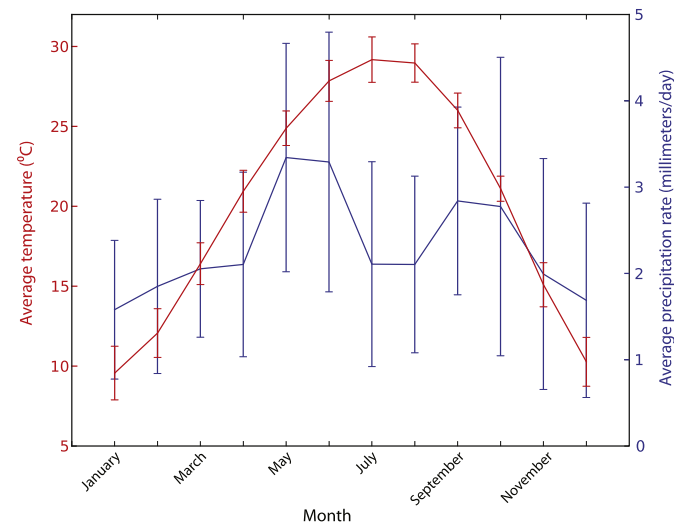


Fig. 1. Monthly temperature and rainfall climatology for Texas illustrating a strong seasonal cycle for temperature whereas precipitation exhibits small intraannual and large interannual variability. The latter is reflected by large error bars in monthly precipitation. Monthly averages calculated from data obtained from Modern-Era Retrospective Analysis for Research and Applications (MERRA; <http://gmao.gsfc.nasa.gov/merra/>) and the Global Precipitation Climatology Project (GPCP; <http://precip.gsfc.nasa.gov/>) for the latitude/longitude range of 28 N, 257E to 34 N, 266E for the interval spanning 1/1/1979 to 12/1/2010. Error bars demarcate two standard deviation (i.e., plus one standard deviation and minus one standard deviation).

2012; van der Ent and Savenije, 2013). These models also document that the northeastern Pacific is a winter-only source. These results are consistent with particle-tracking results indicating that the majority of summer and winter precipitation events in central Texas are associated with air masses with southeast-northwest and northwest-southeast trajectories, respectively (Feng et al., 2014a). Furthermore, forward-tracking and back-trajectory models describe the importance of recycled-continental moisture, which accounts for a greater proportion of precipitation during dry intervals (Dirmeyer and Brubaker, 2007; Gimeno et al., 2012). Quantitative estimates of annual contribution from oceanic sources vs. terrestrial recycling calculated from a water accounting model (van der Ent and Savenije, 2013) over Texas suggest that 23% of precipitation is sourced from the GoM, 9% from the tropical Pacific, 2% from the North Pacific, 5% from the eastern tropical Atlantic, and 29% from terrestrial recycling. The remainder (32%) likely results from more remote oceanic regions (van der Ent and Savenije, 2013).

Developing an understanding of processes governing precipitation extremes across the continental U.S. is a topic of much interest. Many studies have focused on land-sea connections, investigating the degree to which the El Niño/La Niña phases of the El Niño Southern Oscillation (ENSO) and warm/cold phases of the Pacific Decadal Oscillation (PDO) and Atlantic Meridional Oscillations (AMO) coincide with regional moisture extremes (Dong and Sutton, 2007; Feng et al., 2010; McCabe et al., 2008). In general, drier conditions occur across the southwestern and central U.S. during La Niña events due to the northward displacement of the Pacific winter storm track and a summer circulation regime that suppresses convective activity, respectively. The opposite occurs during El Niño events (Seager et al., 2010; Hu and Feng, 2001a). Not all La Niña events, however, induce droughts and not all droughts coincide with La Niña events, which indicates that ENSO effects are likely competing with those from other interannual oscillations (e.g., Arctic Oscillation, North Atlantic Oscillation) and may only be realized in a particular atmospheric state (Hu and Feng, 2001b; Feng et al., 2010).

Variations in large-scale circulation patterns occur on multi-decadal timescales, as modulated by the PDO and AMO. For example, ENSO effects on North American summer precipitation are reduced or absent, depending on region, during a warm PDO phase and are strengthened during the cold phase (Gershunov and Barnett, 1998; Hu and Feng, 2001b). Similarly, ENSO variability is dampened during the warm phase of the AMO, and enhanced during the cold phase (Dong and Sutton, 2007; Dong et al., 2006; Timmermann et al., 2007). Furthermore, the majority of spatial and temporal drought variability across the contiguous U.S. could be attributed to co-variation of the PDO and AMO (McCabe et al., 2004). The PDO acts as a modifier of AMO drought mode, focusing drought over the northwestern U.S. during a positive AMO/PDO and to the southwestern U.S. during a positive AMO/negative PDO (McCabe et al., 2008).

Applying lessons learned from investigations of the spatiotemporal variability of drought throughout the contiguous U.S. to Texas is difficult because no dominant climate process governs precipitation in the State. The much larger interannual, relative to intra-annual, variability in Texas precipitation (Fig. 1) reflects the blend of processes governing rainfall variability to the arid southwestern U.S. and more humid Great Plains and southeastern U.S. This means that Texas hydroclimate is influenced by the modulation of the Pacific winter storm track by ENSO and PDO, and the modulation of the low-level jet and southerly moisture transport in the spring by the AMO (Fig. 2 and Supplemental Fig. 1). With respect to the latter, the North Atlantic Subtropical High is enhanced during the cold (negative phase) of the AMO. This draws low-level southerly flow from the GoM to the continent and drives the formation of an upper-tropospheric front, resulting in more precipitation over most of North America (Hu et al., 2011). Additionally, both the PDO and AMO can enhance or dampen ENSO variability, and thereby have an indirect influence on winter hydroclimate. Lastly, previous work indicates that antecedent moisture conditions and terrestrially recycled moisture likely play a role in the onset, severity, and persistence of drought conditions. Such work has demonstrated (i) a strong coupling between soil moisture and precipitation (Koster et al., 2004), (ii) that dry antecedent moisture conditions (i.e., low soil moisture) enhance convective inhibition, and serve as a positive feedback on summer drought conditions (Myoung and Nielsen-Gammon, 2010), and (iii) interannual variability (2–10 years) of hydroclimate over western North America can be accounted for by local autocorrelation, indicating that persistence of drought indicators (e.g., the Palmer Drought Severity Index [PDSI], soil moisture, tree rings) might not entirely reflect remote forcing (Ault et al., 2013).

3. Methods

Speleothem NBJ was collected from Natural Bridge Caverns (29.69°N, −98.34°W; Fig. 3), which formed in the Cretaceous carbonates of the Edwards Plateau (Small and Hanson, 1994); the Caverns have a lateral extent of 1160 meters (m) and maximum depth of 75 m (Elliott and Veni, 1994). The cave is located where the climate regime transitions from sub-humid to semi-arid, and average annual rainfall is 740 mm with a range from 250 to 1320 mm (1856–2008; Wong et al., 2011). The surface above the Caverns is covered with thin (<30 cm) clay-rich mollisols and juniper, oak, savanna grasses, and cacti (Cooke et al., 2007). Controls on the present day cave environment have been previously investigated (Banner et al., 2007; Breecker et al., 2012; Pape et al., 2010; Meyer et al., 2014; Musgrove and Banner, 2004; Wong et al., 2011).

Stalagmite NBJ was actively growing when collected in 1986 prior to an expansion of the commercial portion of the cave. NBJ is

22 cm long and 7 cm in diameter, and is generally symmetrical along the growth axis. The mineral structure is consistent throughout the sample, based on visual analysis of slabs and thick sections, except for near the top and bottom, where layers of white calcite occur intermittently with layers of clear calcite, and there are thin, dark horizons that are irregularly-spaced.

Calcite powder (0.5–0.8 g) for U-series (U–Th) dating was obtained using a handheld dental drill from select horizons. Calcite powder (~100 µg) for stable isotope analyses ($\delta^{18}\text{O}$ and $\delta^{13}\text{C}$) was collected from the opposite face using a microdrill capable of stepping at 60 µm increments. Following a coarse-scale reconnaissance sampling of 1 mm every 6 mm, samples were drilled from 7 overlapping transects along the speleothem growth axis at increments ranging from 0.1 to 1 mm steps (Supplemental Fig. 2). For U–Th dating, calcite powder was dissolved, and U and Th isolated, following the methods of Edwards et al. (1987, 1993), Cheng et al. (2000), and Musgrove et al. (2001). U and Th separates were loaded onto Re filaments and analyzed using a Thermo Scientific Triton Thermal Ionization Mass Spectrometer within the Department of Geological Sciences (DGS) at The University of Texas at Austin (UT) following the methods of Musgrove et al. (2001). For stable isotope analyses, 30–80 µg aliquots were analyzed using a Thermo MAT253 with a Kiel IV Carbonate Preparation Device within the Austin Laboratory for Paleoclimate Studies in the DGS at UT. Analytical uncertainty is ± 0.06 for $\delta^{18}\text{O}$ and ± 0.03 for $\delta^{13}\text{C}$ based on the standard deviation of 61 replicate analyses of standard NBS19 (National Institute of Standards and Technology [NIST] standard). NBJ $\delta^{18}\text{O}$ and $\delta^{13}\text{C}$ results are reported relative to Vienna Pee Dee Belemnite (VPDB).

Trace-element concentrations (Mg, Sr, Ba) were measured in parts per million (ppm) from four thick sections obtained along the growth axis. Measurements were made in situ using a New Wave Research UP193fx (193 nm, 4–6 ns pulse width) Excimer laser ablation system with a large format (two-volume ablation) cell coupled to an Agilent 7500ce inductively coupled mass spectrometer (DGS at UT). Continuous single tracks along each thick section were pre-ablated and sampled at 15% laser power (1.9 J/cm²), 15 Hz repetition rate, 25 µm/s scan rate, 250 mL/min He flow rate, and 0.31 sampling period with a 25 × 150 µm rectangular slit. The U.S. Geological Survey standard MACS3 (synthetic aragonite) and NIST standard 610 (glass) were analyzed along with the unknowns for elemental quantification. Following background subtraction, concentrations were derived using lolite software (Paton et al., 2011).

An age model was calculated based on U-series ages (n = 13) using the StalAge algorithm developed by Scholtz and Hoffman (2011) (Supplemental Fig. 3). NBJ sampling depths were converted to ages using the resulting age model, and $\delta^{18}\text{O}$, $\delta^{13}\text{C}$, and Mg, Sr, and Ba concentration time-series data were interpolated to 30-year time steps.

4. Results

The growth rate for NBJ ranged from 0 to 90 micrometers per year (µm/yr), with fastest growth rates occurring from 300 to 150 years ago (90 µm/yr) and 5.5 to 5.0 ka (50 µm/yr) (Fig. 4). These values are similar to central Texas speleothem growth rates during the late Pleistocene (Feng et al., 2014a) and last glacial and previous interglacial intervals (Musgrove et al., 2001). Growth rate during the mid Holocene (40 µm/yr) was slightly faster than during the transition to the late Holocene (30 µm/yr). A hiatus in growth from 1.6 to 0.3 ka (Fig. 4) might indicate the driest conditions of the last 7,000 years. This dry interval spans the entirety of the Medieval Climate Anomaly (950–1250 C.E.) and most of the Little Ice Age (1400–1700 C.E.) (Mann et al., 2009), providing some information

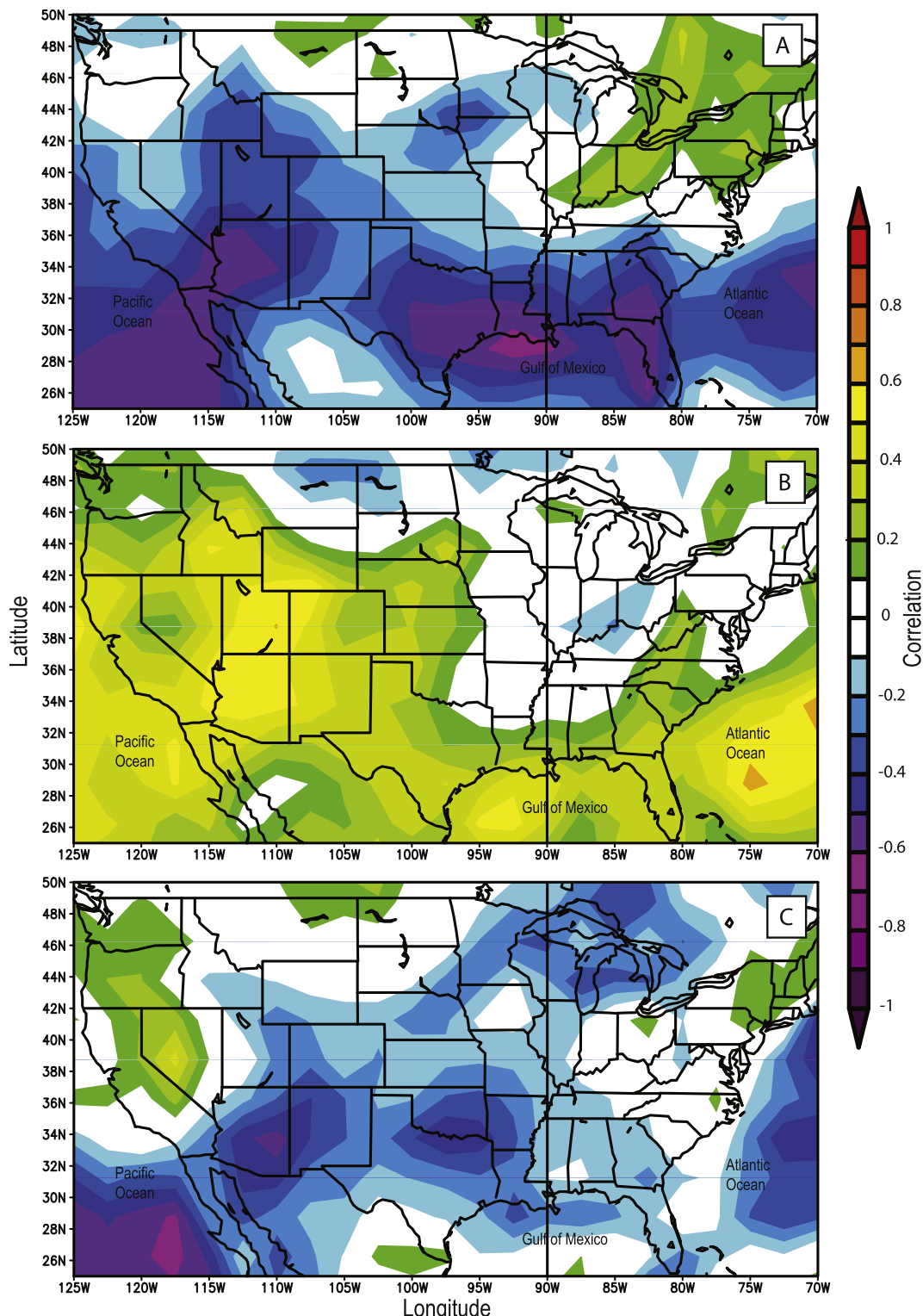


Fig. 2. Correlation between precipitation (Global Precipitation Climatology Project) and the Southern Oscillation Index (SOI; A), Pacific Decadal Oscillation (B), and Atlantic Meridional Oscillation (C) for the interval of 1979–2013. El Niño and La Niña episodes correspond with negative and positive SOI values, respectively. Data from National Oceanic & Atmospheric Administration, Earth Systems Research Laboratory. (www.esrl.noaa.gov/psd/data).

about the nature of Texas climate during these events. Speleothem growth re-initiated toward the end of the Little Ice Age.

NBJ $\delta^{18}\text{O}$ and $\delta^{13}\text{C}$ values range from -4.9 to $-3.6\text{\textperthousand}$ and -8.0 to $-2.7\text{\textperthousand}$, respectively, and are not correlated (except for a brief interval following the growth hiatus) (Fig. 4). There is good

correspondence between vertically overlapping portions of laterally offset transects. The lack of correlation between $\delta^{18}\text{O}$ and $\delta^{13}\text{C}$ values and correspondence between offset transects are consistent with speleothem growth occurring under equilibrium conditions. The strong, positive correlation between $\delta^{18}\text{O}$ and $\delta^{13}\text{C}$ values over

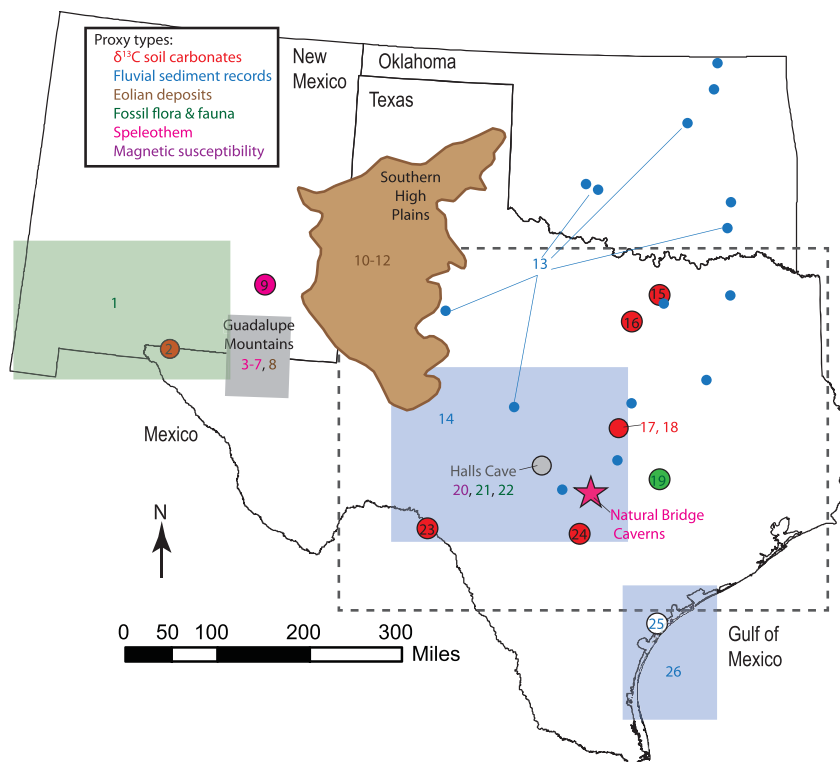


Fig. 3. Locations and study areas of existing Holocene climate reconstructions (Table 1, Fig. 6) along with Natural Bridge Caverns from which speleothem NBJ was collected. Numbers correspond to studies detailed in Table 1. Shaded polygons delineate the study area of the corresponding proxy records. Gray dashed rectangle delineates area for which the modern climatology (Fig. 1) and transient model results (Fig. 9) are calculated.

the short interval (<50 years) following the growth hiatus might reflect calcite deposition under non-equilibrium conditions. That is, kinetic fractionation associated with rapid CO_2 degassing and calcite precipitation may be responsible for the enrichment of $\delta^{18}\text{O}$ and $\delta^{13}\text{C}$ values (e.g., Mickler et al., 2006, 2004). Environmental changes, however, could also result in coincident increases in both $\delta^{18}\text{O}$ and $\delta^{13}\text{C}$ values (e.g., Dorale et al., 1998; Genty et al., 2003). In cases in which it is possible that environmental changes drive co-variation in speleothem $\delta^{18}\text{O}$ and $\delta^{13}\text{C}$ values, it is difficult to discern between the two possible explanations for positively correlated speleothem $\delta^{18}\text{O}$ and $\delta^{13}\text{C}$ values, and paleoclimate interpretations should consider both possibilities (Mickler et al., 2006, 2004). Given that $\delta^{18}\text{O}$ and $\delta^{13}\text{C}$ values do not correlate over most of record, the strong correlation over this brief interval likely indicates an appreciable change in climatic conditions.

NBJ $\delta^{18}\text{O}$ values do not exhibit a temporal trend from the mid to late Holocene, and, instead, regularly fluctuate at a periodicity of 1500 years prior to the hiatus in growth (Fig. 4 and Supplemental Fig. 4). Spectral analysis using a Blackmann-Tukey Fast Fourier Transform, Maximum Entropy Method, Multi-taper Method (MTM), and Singular Spectrum Analysis (SSA) with Monte Carlo significance testing delineates peaks with periods of 1,500, 300 and 130 years. Peaks are significant with respect to red noise background at the 95% confidence interval in both MTM and SSA analyses (Ghil et al., 2000) (Supplemental Fig. 4). The delineation of these spectral peaks by all four techniques indicates that these cycles are a real part of the variability preserved in the sample. The sensitivity of these analyses to age-model uncertainty was evaluated by computing spectra from the median (and also most probable) of 10,000 age-model realizations following the methods of Partin et al. (2013).

NBJ $\delta^{13}\text{C}$ values undergo a +3‰ shift from ~5.5 to 4 ka, and decrease by 1‰ between 4 and 2 ka. Following the hiatus, $\delta^{13}\text{C}$

values rapidly drop from -3 to -8‰ (Fig. 4). $\delta^{13}\text{C}$ values are more variable during the mid Holocene (~6 ka) than during the transition from the mid to late Holocene.

NBJ trace-element concentrations and variability (Mg, Sr, Ba) correlate with each other (Supplemental Fig. 5), but do not co-vary with isotopic variations. Because trace-element variability is similar, figures includes only Sr concentrations for discussion of results. Similar to $\delta^{18}\text{O}$ values, trace-element concentrations do not exhibit a temporal trend from the mid to late Holocene. Unlike the regular periodicity of variation in $\delta^{18}\text{O}$ values, however, spectral analysis did not delineate statistically significant periodicity in trace-element variability. Similar to $\delta^{13}\text{C}$ values, trace-element concentrations exhibit anomalous variability, relative to the rest of the record, following the growth hiatus when concentrations rapidly decrease to their lowest values (Fig. 4).

5. Non-trending, centennial variability in mid to late Holocene moisture conditions

Speleothem trace-elements are commonly interpreted to reflect relative moisture conditions (e.g., Johnson et al., 2006; Cruz et al., 2007; Oster et al., 2009). In present day cave environments, variations in drip water trace-element concentrations (relative to Ca concentrations) reflect relative moisture conditions via two processes—water interaction with the host rock (water–rock interaction, WRI) and calcite precipitation from drip water prior to its deposition on the speleothem of interest (prior calcite precipitation, PCP) (e.g., Fairchild et al., 2000; Johnson et al., 2006; Fairchild and Treble, 2009; Matthey et al., 2010; Oster et al., 2012; Sinclair et al., 2012; Tremaine and Froelich, 2013). Multiple studies have demonstrated that these processes dictate drip water trace-element ratios in central Texas caves (Musgrave and Banner, 2004; Wong et al., 2011; Casteel and Banner, 2015). Furthermore,

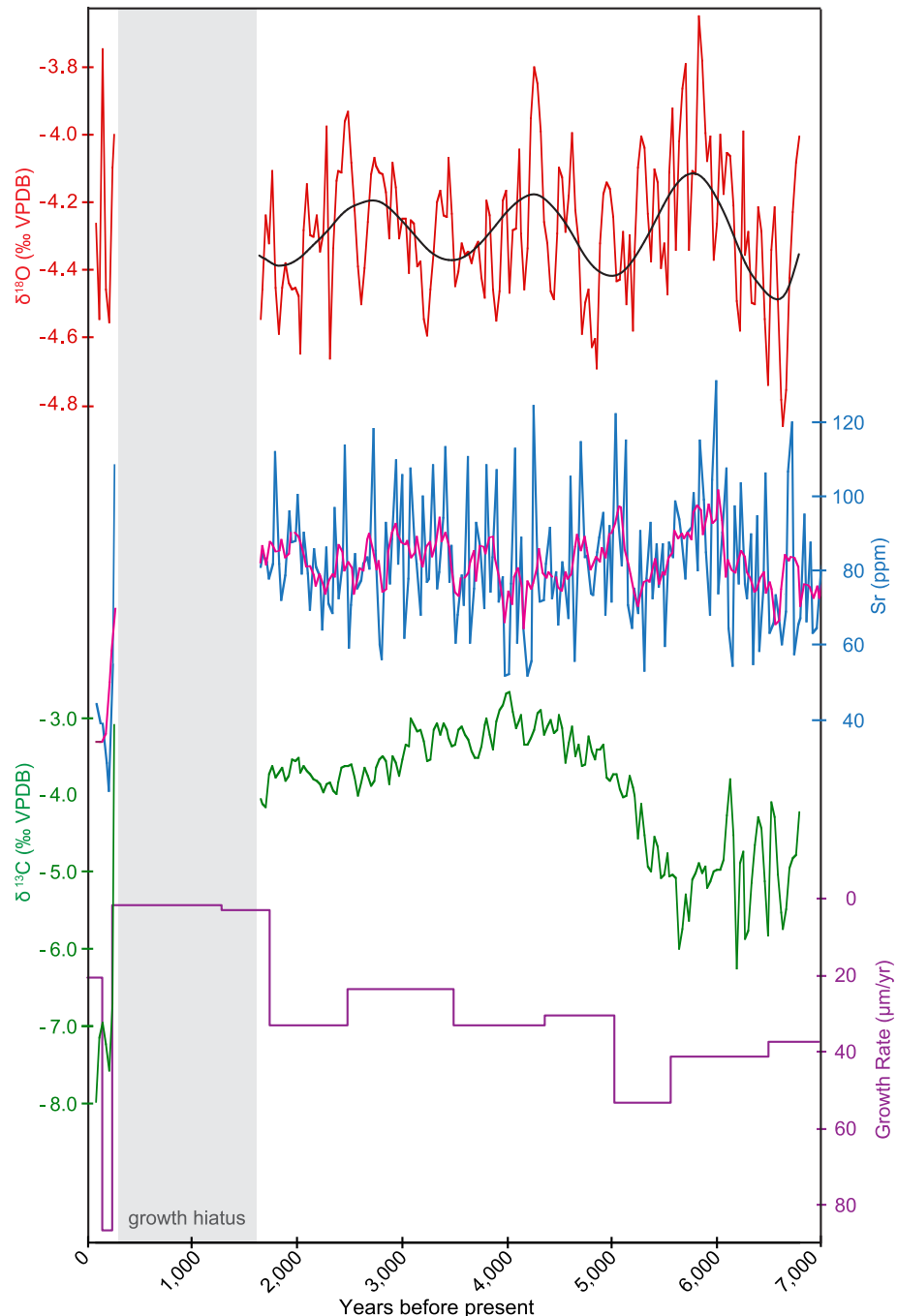


Fig. 4. NBJ speleothem $\delta^{18}\text{O}$ (red), Sr concentrations (blue), $\delta^{13}\text{C}$ (green) values, and growth rate (purple). $\delta^{18}\text{O}$ and $\delta^{13}\text{C}$ values and Sr concentrations interpolated to 30 year intervals. The leading component of variability (black) (1500 yr) of the $\delta^{18}\text{O}$ time series, delineated by single-spectrum analysis (see *Supplemental Fig. 4*), accounts for 25% of the variation. Pink curve (5-point smooth of the 30-yr Sr concentration) shows lower frequency variability. Growth rate axis is inverted.

the slope of the relation between $\ln(\text{Mg/Ca})$ and $\ln(\text{Sr/Ca})$ (and $\ln(\text{Sr/Ca})$ and $\ln(\text{Ba/Ca})$) provides a theoretically-based diagnostic of the potential role of WRI and PCP (Sinclair et al., 2012). The slope for the relation between $\ln(\text{Mg/Ca})$ and $\ln(\text{Sr/Ca})$ is 0.42, which falls within the calculated range of slopes (0.18–0.53) that would result from calcite recrystallization (Sinclair et al., 2012). The slope for the relation between $\ln(\text{Sr/Ca})$ and $\ln(\text{Ba/Ca})$ is 0.99 (Casteel and Banner, 2015), which is similar to the calculated range of slopes (0.91–0.99) that would result from PCP. In most caves, the extent to which WRI and PCP occur is influenced by the duration of water transit through the vadose zone, such that trace-element ratios are

higher under drier conditions and lower under wetter conditions. The extent of PCP can also vary seasonally at sites in which cave-air pCO_2 reaches levels that slow calcite growth (e.g., Banner et al., 2007; Baldini et al., 2010; Mattey et al., 2010; Wong et al., 2011). Additionally, a recent study suggests that the extent of PCP that occurs can be related to temperature at sites near well-ventilated cave openings experiencing seasonal temperature variability (Casteel and Banner, 2015).

Acknowledging the complexity of the cave system and multiple possible controls of speleothem trace-element concentrations, we interpret variations in NBJ trace-element concentrations to reflect

relative changes in moisture conditions based on several considerations. NBJ was collected at a depth of 40 m with ~100 m of narrow passage from the natural cave opening. The distance from the cave opening and the lack of seasonal temperature variation in the present day regime (Wong et al., 2011) indicate that temperature is an unlikely control on the extent of PCP. Rather, Wong et al. (2011) demonstrated that drip water trace-element ratios were controlled by WRI and PCP processes related to changes in moisture conditions and seasonal cave ventilation. It is likely, however, that multi-decadal variations in NBJ trace-element concentrations reflect changes in moisture conditions. Variations in moisture conditions dictate the degree to which subsurface voids are filled with water or air influencing both (i) the duration of water transit time from the surface to the stalagmite, and, consequently, the amount of WRI and PCP that can occur, and (ii) the degree of ventilation in subsurface voids influencing the amount of PCP that can occur (e.g., Musgrove et al., 2004; Johnson et al., 2006; Mathey et al., 2010; Wong et al., 2011).

The cave is seasonally ventilated, which means that its speleothems might contain a bias towards winter conditions (Banner et al., 2007). Texas moisture conditions, however, are strongly influenced by antecedent moisture conditions and droughts can span multiple years (Koster et al., 2004; Myoung and Nielsen-Gammon, 2010; Ault et al., 2013). It is likely that winter-only deposition reflects antecedent moisture conditions (i.e., moisture conditions from earlier in the year or from the previous year) as the saturation state of the vadose zone above the cave is sensitive to antecedent moisture conditions and influences drip water trace-element ratios. Therefore, we interpret multi-decadal variations in NBJ trace-element concentrations to reflect non-trending, but oscillating mid to late Holocene moisture conditions (Fig. 4).

6. NBJ growth rates and $\delta^{13}\text{C}$ values as a proxy for changes in ecosystem processes

The co-variation of NBJ growth rates, $\delta^{13}\text{C}$ values, and trace-element concentrations provides insight into processes most likely controlling how each proxy is linked to climate variability. Trace-element concentrations do not co-vary with $\delta^{13}\text{C}$ values or growth rates, but there is a synchronous shift in $\delta^{13}\text{C}$ values and growth rates (Fig. 4). This suggests that $\delta^{13}\text{C}$ values and speleothem growth rates most likely reflect combined variations in temperature and moisture conditions as modulated by the ecosystem overlying the cave.

Drip water $\delta^{13}\text{C}$ values are influenced by WRI and PCP in a similar manner as drip water trace-element ratios (i.e., higher values occur under drier conditions) (e.g., Baker et al., 1997; Genty et al., 2001; Fairchild et al., 2006; Spotl et al., 2005). Two additional processes can also govern drip water $\delta^{13}\text{C}$ values: (i) the contribution of respiration CO₂ from the soil zone (Genty et al., 2003; Oster et al., 2010; Breecker et al., 2012; Meyer et al., 2014), and (ii) the proportion of cool/wet adapted-C₃ vs. warm/dry adapted-C₄ vegetation (e.g., Dorale et al., 1998; Hellstrom et al., 1998; Bar-Matthews et al., 1999; Denniston et al., 2007). Both these ecosystem related processes are influenced by both temperature and moisture conditions, such that higher $\delta^{13}\text{C}$ values occur during warmer/drier conditions. Additionally, neither the contribution of soil respiration CO₂ nor the proportion of C₃–C₄ vegetation have been demonstrated to strongly influence dripwater trace-element ratios (Cruz et al., 2007). This indicates that the nature of co-variation between speleothem $\delta^{13}\text{C}$ values and trace-element ratios might be a potential indicator of the relative influence of factors controlling $\delta^{13}\text{C}$ values that are dominantly moisture related vs. those mediated by the overlying ecosystem (Cruz et al., 2007). In application, the contrasting nature of variability in $\delta^{13}\text{C}$ values and trace-

element ratios from the mid to late Holocene (Fig. 4) combined with the dominant control of moisture-related processes on trace-element concentrations, indicates that $\delta^{13}\text{C}$ values likely reflect ecosystem processes. Thus, we interpret a rapid increase in $\delta^{13}\text{C}$ values around 5 ka to reflect a shift in ecosystem composition or productivity.

The timing of the shift in $\delta^{13}\text{C}$ values around 5 ka (Fig. 4) is consistent with the establishment of present-day soil conditions following the progressive denudation of the landscape at a constant erosion rate over the previous 16 ka interval (Cooke et al., 2003). This prompts the hypothesis that ecosystem characteristics controlling speleothem $\delta^{13}\text{C}$ values responded rapidly once a certain soil depth threshold was breached. This is consistent with Breecker et al. (2012), who demonstrate that C₃ trees can comprise the dominant supply of CO₂ to Texas caves even when sparsely present. This means that speleothem $\delta^{13}\text{C}$ values are likely biased toward any deeply rooted vegetation that is present. The shift in NBJ $\delta^{13}\text{C}$ values from 5.5 to 5.0 ka, therefore, might represent the transition when deeply rooted C₃ trees became sufficiently sparse and shallowly rooted C₄ grasses became sufficiently abundant and contiguous to overcome the bias. Alternatively, it could reflect a drastic reduction in soil/vadose zone CO₂ productivity with the establishment of the present day soil mantle.

Evaluation of co-variation of NBJ growth-rate variations with trace-element concentrations and $\delta^{13}\text{C}$ values indicates that growth-rate variations likely reflect combined temperature-moisture variability rather than moisture alone. Speleothem growth rates can be dominated by water supply (e.g., Banner et al., 2007; Dreybrodt, 1999) and are generally used as a coarse proxy for moisture conditions (e.g., Musgrove et al., 2001; Polyak et al., 2004). Faster NBJ growth rates from 7 to 5 ka (during the mid Holocene), relative to later (<5 ka), however, contrast with non-trending trace-element concentrations (Fig. 4). Speleothem growth rates can additionally be influenced by (i) the effect of soil CO₂ concentrations on the saturation state of infiltrating water with respect to calcite (i.e., Ca concentrations), and (ii) cave-air CO₂ concentrations that dictate the rate at which CO₂ degasses from drip water upon entering the cave (e.g., Banner et al., 2007; Baldini et al., 2010). Typically, greater ecosystem productivity, as influenced by a variety of factors (e.g., temperature, moisture, ecosystem composition, and disturbance), results in higher soil CO₂ concentrations that increase the saturation of dripwater with respect to calcite and, consequently, calcite precipitation rates (Baldini, 2010; Oster et al., 2010). Conversely, seasonal cessation of temperature-related, density-driven ventilation of the cave atmosphere can lead to a buildup of cave-air CO₂. When cave-air CO₂ reaches sufficiently high concentrations, the degassing of CO₂ from cave drip water and subsequent calcite deposition is inhibited (Banner et al., 2007). As soil CO₂ is a primary source of cave-air CO₂ (e.g., Genty et al., 2001; Breecker et al., 2012), these two controls can be linked. For example, Wong and Banner (2010) demonstrated that the removal of vegetation above Natural Bridge Caverns resulted in increased calcite growth rates. Reduced calcite growth rates were expected to follow the vegetation removal due to decreased production of soil CO₂. The decreased production of CO₂, however, prevented the buildup of cave-air CO₂ concentrations in the summer (when the cave was not ventilated) that inhibited summer calcite growth prior to the vegetation removal. Year-round calcite growth was, therefore, enabled in a cave that typically experienced a summer pause in deposition.

The potential ecosystem shift ~5 ka, reflected by $\delta^{13}\text{C}$ values, might be responsible for the difference in growth rate between the mid and late Holocene (Fig. 4). The shift from deeply to shallowly rooted vegetation would have been associated with decreased soil CO₂ production (Breecker et al., 2012; Wong and Banner, 2010). This

reduction may be responsible for damped speleothem growth rates, caused by decreased saturation of dripwater with respect to calcite, in the late Holocene relative to mid Holocene (Fig. 4). A reduction in soil CO₂ production that lowered summer cave-air CO₂ concentrations would have resulted in year-round growth and higher, not lower, speleothem growth rates. This indicates that growth-rate variations might reflect changes in soil CO₂ production related to a change in the ecosystem overlying the cave rather than changes in seasonal ventilation.

7. Decoupling of moisture source and moisture amount

NBJ δ¹⁸O variations are distinct from trace-element concentrations, indicating that δ¹⁸O variations might reflect a unique climate process that is decoupled from moisture amount. Trace-element concentrations indicate frequent cycling between wet and dry conditions, with slightly prolonged dry intervals occurring between 7 and 4 ka (Fig. 4). There is poor correspondence, however, between δ¹⁸O and trace-element variations throughout the mid to late Holocene. This decoupling indicates either that (i) variations in moisture source likely have subtle, if any, influence on relative moisture conditions, or (ii) NBJ trace-element concentrations are not a direct or sensitive proxy of moisture conditions. With regard to the latter, present-day cave monitoring studies have demonstrated that drip water trace-element response to changes in rainfall, and(or) drip rate, or both can be variable between caves as well as between sites within the same cave (Karmann et al., 2007; McDonald et al., 2007; Wong et al., 2011). With regard to the former, an assessment of more than a decade of drip water and rainfall δ¹⁸O monitoring in central Texas indicates that rainfall and speleothem δ¹⁸O variations reflect the relative proportion of Pacific-vs. GoM-derived and(or) terrestrially recycled moisture (Pape et al., 2010; Feng et al., 2014a; Supplemental Material; Supplemental Fig. 6). An assessment of present day precipitation dynamics, however, found similar interannual variability in summer precipitation regardless of the driving climate process (ENSO or southerly flow from the GoM) responsible for such variability (Hu and Feng, 2001b).

Decoupling between speleothem δ¹⁸O values and other moisture proxies in the region has previously been documented, but not discussed. There is little correspondence between δ¹⁸O values and growth rate for a speleothem (PP1) from Pink Panther Cave in the Guadalupe Mountains in New Mexico, even though the δ¹⁸O values are interpreted to reflect precipitation amount (Asmerom et al., 2007) (Fig. 5). There is, however, striking similarity between NBJ and PP1 growth rates. The apparent decoupling between δ¹⁸O values and growth rate in PP1 might be (i) an artifact of few age constraints with relatively large uncertainties, (ii) a result of speleothem growth being a proxy of soil CO₂ production affected by both temperature and moisture conditions, as might be the case with NBJ, or (iii) independent of climate processes governing moisture source and precipitation amount as speleothem δ¹⁸O values in this region can also be interpreted as a changing proportion of Pacific-vs. GoM-derived moisture (Asmerom et al., 2010; Wagner et al., 2010; Feng et al., 2014a). It is difficult to assess which possibility is most likely because other speleothem proxy data (δ¹³C values and(or) trace-element concentrations) for PP1 are not available. The poor correspondence between NBJ and PP1 δ¹⁸O values despite the similarity in speleothem growth rate supports the third hypothesis.

The δ¹⁸O values in speleothems from both southeastern New Mexico and central Texas have been interpreted to reflect the proportion of Pacific-vs. GoM-derived moisture (Asmerom et al., 2010; Feng et al., 2014a). This interpretation is consistent with a gradient of decreasing δ¹⁸O values between Texas and Arizona

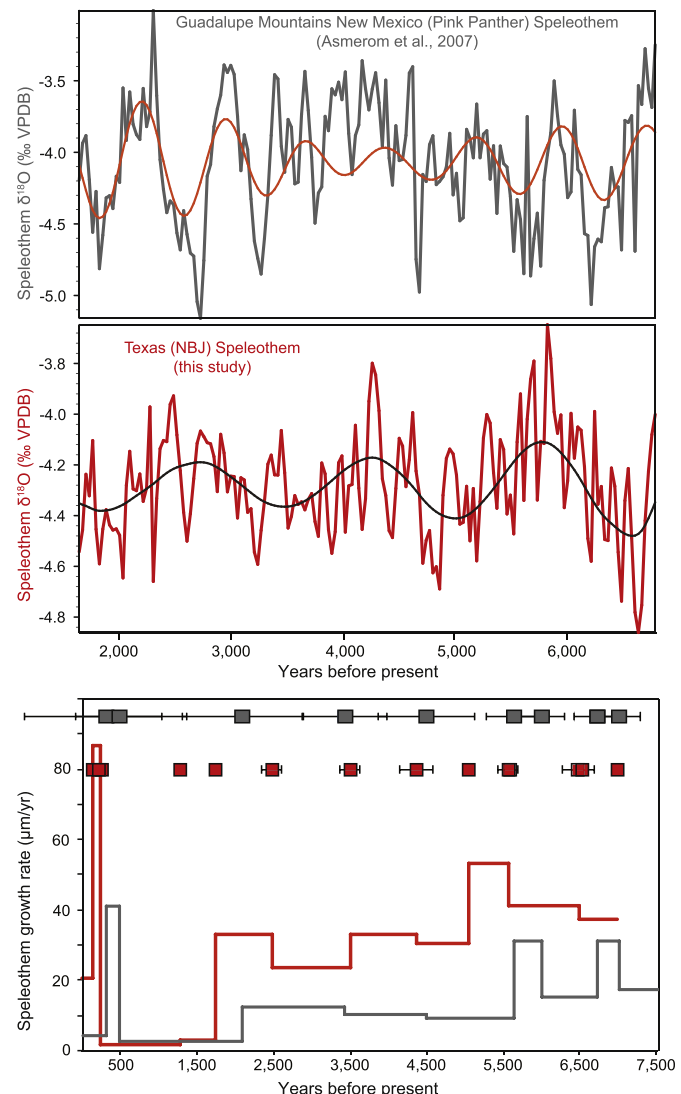


Fig. 5. Texas (red) and New Mexico (gray) speleothem δ¹⁸O and growth-rate time series. Orange and black curve show model δ¹⁸O based on the ~1500 year and ~700 cycle identified in the spectral analysis of each time series that account for the 25%, and 29%, respectively, of the variance. Speleothem age constraints (U-Th) and uncertainty delineated as squares.

during the late Pleistocene that reflects the progressive diminishment of GoM-derived moisture with proximity to the GoM. However, the climate processes governing moisture transport to Texas and New Mexico are quite different. Pink Panther Cave in New Mexico is affected by the North American Monsoon (NAM), and receives NAM-associated moisture derived from the Gulf of California, GoM, and tropical Pacific during the early and mid summer (Higgins, 1997). Moisture derived from the Gulf of California and tropical Pacific would produce precipitation with δ¹⁸O values higher than those measured for precipitation associated with the winter Pacific westerly storm track that transports moisture from the North Pacific to the contiguous U.S. (Berkelhammer et al., 2011). Precipitation in central Texas draws on GoM-derived moisture year-round, with the greatest contributions associated with the Great Plains Low-Level jet in the spring. It is, therefore, reasonable to expect a contrast between NBJ and PP1 δ¹⁸O values given the distinct nature of the climate processes contributing GoM-derived moisture to southeastern New Mexico and central Texas.

Lastly, it is interesting to note the difference in magnitude of the typical δ¹⁸O oscillations in the two records – a moving window of

0.8‰ captures nearly all the variability in the NBJ record, whereas a window of 1.5‰ captures the same for PP1. The magnitude of variability for each is similar in additional speleothem $\delta^{18}\text{O}$ records from Texas (CWN-4; Feng et al., 2014a) and New Mexico (FS-2; Asmerom et al., 2010) that grew during the deglaciation (~20–11 ka). The absolute $\delta^{18}\text{O}$ values, however, are distinct between the two regions during the deglaciation (~8‰ in New Mexico and ~4‰ in Texas), but similar during the Holocene (~4‰). The 4‰ increase in $\delta^{18}\text{O}$ values in New Mexico during the deglaciation may reflect the growing influence of the NAM during the Holocene in New Mexico relative to Texas, as NAM-related, summer precipitation is isotopically enriched relative to winter precipitation.

8. NBJ in the context of existing paleoclimate data

A transition from a generally wetter Pleistocene to a drier Holocene is well documented for the southwestern U.S. (e.g., Asmerom et al., 2010; Wagner et al., 2010; Feng et al., 2014a). Variability within the Holocene, which was stable relative to the earlier glacial period and glacial-to-Holocene transition, is less well defined, and is challenging to determine because of discontinuous proxy records, limited age constraints, and contrasting interpretations. We synthesize published interpretations of available proxy records from in and near Texas to provide an overview of the evolution of Holocene climate (Figs. 3 and 6, Table 1).

All of the proxy records are interpreted as a response to moisture conditions or an integrated response to moisture and temperature conditions (with wet conditions generally corresponding with cooler temperatures, and dry conditions corresponding with warmer temperatures); none of the proxy records pertain solely to temperature. For comparison purposes, we integrate moisture and temperature responses (Fig. 6), but clarify each record's focus in Table 1. None of the existing paleoclimate records provide quantitative indicators of the magnitude of changes; rather the variability described is generally qualitative, often relative to changes

observed in the individual records and(or) relative to present-day conditions. Since all of the existing records are qualitative, we use a categorization scheme to identify similar trends, as originally interpreted by the respective authors, in records of varying proxy types as follows (i) "warm/dry" reflect intervals interpreted, by the original authors, to reflect warmest and(or) driest Holocene conditions, (ii) "warming/drying" reflect transitional intervals leading up to peak warm/dry conditions, and (iii) "cool/wet" reflect persistent intervals of cool/wet conditions in the early Holocene that followed the culmination of such conditions in the Late Pleistocene, or a reversal of mid to late Holocene warm/dry conditions (Fig. 6).

The synthesis reveals that there is considerable variability among the different records (Fig. 6), which are all indirect climate measures and may have a complex response to climate variability and(or) exhibit temporal lags in that response. Proxy records may not be stratigraphically continuous, resulting in sporadic records, such as studies of aeolian activity (Rich and Stokes, 2011; Holliday, 2001), fluvial channel trenching (Hall, 1990), and packrat middens (Holmgren et al., 2007). For many proxies, there are few geochronological controls, ages might have large errors, or specific material is required for dating. Relatively small-scale climate variability may result in substantial landscape effects, leading to challenges in proxy interpretation (for example, Holliday, 2001). Climate may be only one of many factors affecting landscape change, which complicates interpretation of proxies such as fluvial geomorphology (Waters and Nordt, 1995) or vegetation distribution (Holmgren et al., 2003).

Many regional Holocene climate reconstructions are based on interpretations of $\delta^{13}\text{C}$ variations in paleosols and buried soil sequences (Fig. 3, Table 1). These proxies tend to preserve climate variability influenced by both temperature and moisture, meaning that distinguishing the relative influence of each necessitates comparison with independent, temperature- or moisture-exclusive proxies. Furthermore, these records are often irregularly

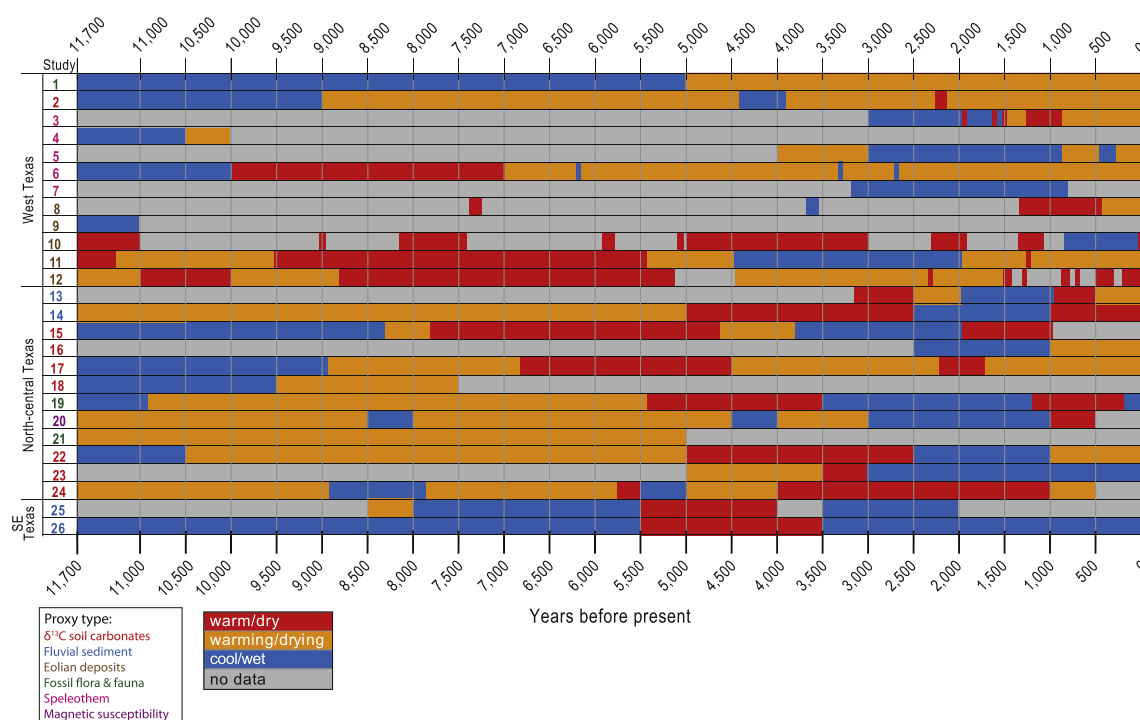


Fig. 6. Summary of Holocene climate from the literature. Orange = warming/drying; red = warmest/driest; blue = cool/wet. Study number corresponds to those in Fig. 3 and Table 1. Color of study number reflects proxy type. Studies detailed in Table 1.

Table 1

Summary information for paleoclimate proxy studies in and near Texas.

Study	Proxy ^{b,c}	Location	Age (ka)	Age Model	Notes
1. Holmgren et al., 2007	^b Vegetation in packrat middens	Chihuahuan Desert (TX, NM, northern Mexico)	20 to 0	¹⁴ C	Climate inferences from desert grasses and shrubs
2. Buck and Monger 1999	^b Buried soils; geomorphology and $\delta^{13}\text{C}$	Chihuahuan Desert (TX, NM)	19 to 0	¹⁴ C	C_3 -dominant vegetation indicative of desert scrub and aridity
3. Rasmussen et al., 2006	^b Speleothem (band thickness)	Guadalupe Mountains, NM	3 to 0	U-series; annual banding	Decadal-scale spectral peaks related to Pacific-modulated moisture
4. Polyak et al., 2004	^b Speleothem (growth chronology)	Guadalupe Mountains, NM	14.5 to 10	U-series	Limited growth in arid regions related to moisture and drier climate
5. Polyak and Asmerom 2001	^c Speleothem (band thickness and chronology)	Guadalupe Mountains, NM	4 to 0	U-series	Annual banding
6. Asmerom et al., 2007	^b Speleothem ($\delta^{18}\text{O}$)	Guadalupe Mountains, NM	12 to 0	U-series	Link variability in rainfall with solar forcing
7. Polyak et al., 2001	^b Speleothem (mites)	Guadalupe Mountains, NM	3.2 to 0.8	U-series	Presence of mites preserved in speleothems related to climate
8. Wilkins and Currey 1999	^b Dune activity and organic carbon $\delta^{13}\text{C}$	Guadalupe Mountains, NM, TX	7.3 to 0	¹⁴ C ^a	Eolian deposition associated with dry climate
9. Asmerom et al., 2010	^c Speleothem ($\delta^{18}\text{O}$)	Southeastern NM	56 to 11	U-series	Mostly older record but includes Younger Dryas
10. Rich and Stokes 2011	^b Eolian deposits	Southern High Plains; Pecos River Valley, TX, NM	200 to 0	^d OSL; ¹⁴ C (previous studies)	Eposodic eolian deposition and dune activity associated with dry climate
11. Holliday et al., 2008	^b Playa sedimentology and fill	Southern High Plains (TX, NM)	24 to 0	¹⁴ C ^a	Increasing importance of xeric C_4 grasses through the Holocene
12. Holliday 2001	^b Eolian deposits	Southern High Plains (TX, NM)	13 to 0	¹⁴ C ^a	Minor climate fluctuations can result in substantial landscape impacts
13. Hall 1990	^b Fluvial channel trenching	Southern Great Plains (TX, OK)	3.2 to 0	¹⁴ C ^a	15 alluvial sequences with record of channel trenching
14. Blum et al., 1994	^c Fluvial landscape development	Edwards Plateau - central TX	20 to 0	¹⁴ C, chronostratigraphy	Interpretation reliant on existing climate reconstructions (esp. #22)
15. Humphrey and Ferring 1994	^b Pedogenic/lacustrine carbonates, $\delta^{13}\text{C}$, $\delta^{18}\text{O}$	Aubrey Clovis site, north-central TX	17.4 to 1.5 ^a	¹⁴ C ^a	Southern Great Plains; includes data from Ferring 1990
16. Hall et al., 2012	^c Paleosol, $\delta^{13}\text{C}$	Trinity River basin—central TX	2.3 to 1	¹⁴ C	Contrasting interpretation of $\delta^{13}\text{C}$ values relative to other studies
17. Nordt et al., 1994	^c $\delta^{13}\text{C}$ of soil carbon	Fort Hood Military Reservation, central TX	15 to 0 ^a	¹⁴ C ^a	Summarized in Waters and Nordt 1995
18. Meier et al., 2014	^c $\delta^{13}\text{C}$ of soil carbon, buried soil sequence	Brazos River - central TX	14 to 8	OSL	
19. Boulter et al., 2010	^b Bog pollen and sedimentary sites	Boriak Bog, adjacent sites, east-central TX	19 to 0	¹⁴ C, OSL	Longer record, improved age control relative to Bryant 1977, Bousman 1998
20. Ellwood and Gose 2006	^c Magnetic susceptibility	Halls Cave - central TX	19 to 0.5	¹⁴ C	Interpretation reliant on co-variation with #22 fossil sequence; calendar-age sequence from #21
21. Cooke et al., 2003	^c Sr isotopes of fossil seeds and teeth	Halls Cave - central TX	20 to 1.5	¹⁴ C	Soil erosion driven by increased aridity and increased seasonality and intensity of precipitation
22. Toomey et al., 1993	^c Cave fill sediments (flora and fauna)	Halls Cave - central TX	20 to 0	¹⁴ C	
23. Goodfriend and Ellis 2000	^b $\delta^{13}\text{C}$ of snail shells	Hinds Cave - west TX	5 to 0	¹⁴ C	Largely controlled by snail diet; related to moisture conditions and drought-adapted plants
24. Nordt et al., 2002	^c $\delta^{13}\text{C}$ of soil carbon, buried soil sequence	Medina River valley, south-central TX	24 to 0.5 ^a	¹⁴ C ^a	
25. Troiani et al., 2011	^b Seismic/sediment cores (wind strength)	Copano Bay - south TX coast	8.2 to 0	¹⁴ C, chronostratigraphy	Wind strength correlated with drier climatic conditions as per other records
26. Weight et al., 2011	^c Seismic/sediment cores	Texas Mud Blanket - northwestern Gulf of Mexico	17 to 0	¹⁴ C	Related to sediment input from central Texas streams

^a ^{14}C ages calibrated to calendar ages using Cologne Radiocarbon Calibration and Paleoclimate Research Package (CalPal online): <http://www.calpal-online.de/index.html>.^b Proxy interpretation focused on moisture conditions.^c Proxy interpretation integrates moisture and temperature conditions.^d OSL – optically stimulated luminescence.

discontinuous, fail to preserve the transitional nature between shifts in climate regimes, and can have large uncertainties in their age determinations (usually based on ^{14}C). Interpretation of $\delta^{13}\text{C}$ proxies requires consideration of both climate and biosphere forcings. For example, Hall et al. (2012) propose that wet-meadow biomes, which are characterized by C_4 prairie grasses, expanded under wetter Holocene conditions. This relation (i.e., increasing C_4 abundance with wetter conditions) is contrary to the common interpretation of increasing C_4 abundance reflecting the transition from woodland- (C_3) to grassland-dominated environments (C_4) under drier conditions (e.g., Nordt et al., 2007). Such differences in

interpretation of proxy controls might lead to opposing paleoclimate interpretations. Furthermore, the proportion of C_3 - C_4 vegetation could be influenced by the numbers and types of browsers and grazers, which, in addition to climate, might be affected by the hunting activity of Paleoindians in the region. The use of fire by Paleoindians to actively shape the landscape might also be a non-climate control on vegetation changes (Cordova et al., 2011).

Other regional Holocene climate reconstructions are based on fluvial and geomorphological sediment records (Fig. 3). These are particularly complex and indirect proxies because of the ambiguous

interpretation of climate conditions associated with erosion and deposition (Boulter et al., 2010). Decreasing vegetative cover during drier intervals would enable greater aeolian and colluvial deposition, and the opposite would be expected during wetter intervals. The decrease in deposition associated with increased vegetative cover during wetter intervals, however, could be countered by increased erosive energy associated with more intense and(or) frequent precipitation events. Ambiguities in the interpretation of proxy controls associated with sediment accumulation lend uncertainty to comparisons between such proxies.

In spite of the complexities and challenges of comparing and synthesizing these paleoclimate records, some consistency in climatic conditions is evident (Fig. 6) — a pattern of warming/drying during the transition from the Pleistocene into the middle Holocene; a slight, temporary excursion to cooler/wetter conditions in the late Holocene; and a distinct dry interval within the last two millennia. The early Holocene was relatively wet, transitioning from the last Pleistocene glacial, and conditions became progressively drier into the middle Holocene (Fig. 6). There is discrepancy in the timing of the maximum warm and dry conditions, as some records indicate the drying was earlier (7–5 ka) and others suggest later (5–3 ka) (Fig. 6). A reprieve from this culmination to slightly cooler and wetter conditions follows in the late Holocene (3–1 ka) (Fig. 6), although conditions of the late Holocene remain warmer and drier than the early Holocene (e.g., Toomey et al., 1993; Nordt et al., 2002; Ellwood and Gose, 2006). This reprieve is temporary as many of the records document distinct dry intervals within the last two millennia (Fig. 6). Also worth noting is evidence for frequent cycling between wet and dry conditions throughout the Holocene, despite the overriding warm/dry or cool/wet patterns (e.g., Blum et al., 1994; Boulter et al., 2010; Ellwood and Gose, 2006). Although a general consensus of Holocene climate evolution can be inferred from this compilation, there is uncertainty with respect to the precise timing of climate transitions and the magnitude of temperature and moisture changes.

We consider the NBJ record in the context of existing paleoclimate studies. The lack of a distinct pattern of variation in NBJ trace-element concentrations seems inconsistent with the majority of Holocene reconstructions from the region that indicate climatic transitions between warm/dry and cool/wet conditions in the mid and late Holocene (Fig. 4). The absence of any distinct variation in NBJ trace-element concentrations, however, indicates that existing proxies might dominantly reflect a temperature, as opposed to moisture, signal (although the majority of studies focus on moisture interpretations, rather than temperature). More likely, the apparent discrepancy between the record of NBJ trace-element concentrations and paleoclimate variability indicated by other records could reflect aliasing by the discontinuous and (or) low-resolution nature of existing records, and (or) factors other than moisture conditions influencing NBJ trace-element concentrations. The variation of NBJ $\delta^{13}\text{C}$ values, however, closely resembles the aggregate reconstruction of Holocene conditions from the existing proxy records (Figs. 4 and 6). Highest NBJ $\delta^{13}\text{C}$ values occur between 5 and 3 ka, consistent with other records indicating maximum warm/dry conditions during this interval. Additionally, the NBJ $\delta^{13}\text{C}$ record returns to lower values within the last 3 ka, consistent with cooler and(or) wetter conditions as indicated by other records in the region (Fig. 4).

9. Comparison of high-resolution Holocene records

Previous to NBJ, the most well-dated and detailed records of Holocene climate variability in Central Texas were from Hall's Cave (Table 1, Figs. 3 and 7). Sediments washed into the cave provide a continuous stratigraphic section from which records of flora and

fauna (Cooke et al., 2003; Toomey et al., 1993) and magnetic susceptibility (MS) (Ellwood and Gose, 2006) have been linked to climate variability. The MS record primarily details centennial variation in Holocene temperature, but also preserves large moisture anomalies. Paired with variation in the faunal record interpreted as a moisture proxy, the sediment sequence provides the most resolved timing of Holocene climate.

A preliminary assessment indicates little correspondence between the NBJ speleothem record and the Hall's Cave sediment proxies. Consideration of the nature of each proxy, however, enables coarse reconciliation of the two records with respect to the preservation of (i) a warming trend from the mid to late Holocene, with a slight reprieve to cooler conditions in the late Holocene, (ii) a hiatus in deposition at 1 ka, and (iii) occurrence of anomalous post-hiatus values in both records that are challenging to interpret with respect to climate. The timing of inferred climate variations, however, is offset between the two records (i.e., variability in MS lags NBJ $\delta^{13}\text{C}$ values), which may reflect an age offset between pedogenesis and deposition in the MS record.

A detailed comparison of the NBJ record to Hall's Cave sediments is warranted because (i) these records are the highest resolution available to date in Texas, and (ii) the records, as interpreted, tell somewhat different tales of Holocene climate. Potential controls on speleothem growth rate, $\delta^{13}\text{C}$ values, and trace-element concentrations are discussed above in Sections 5 and 6, and a corresponding understanding of sediment MS is warranted. MS is based on the production of magnetite or maghemite in soils, which is controlled by both temperature and moisture conditions such that the greatest production occurs under *warm and wet* conditions (Ellwood and Gose, 2006). Although temperature is the dominant factor driving pedogenesis, climate interpretations can be ambiguous as past warm intervals have typically been associated with *dry* conditions. For example, increases in Hall's Cave MS at 17 and 8.2 ka were interpreted as shifts to warmer/drier climates, whereas the increase in MS values occurring at 4.4 ka was interpreted as a shift to wetter conditions (Ellwood and Gose, 2006). Furthermore, MS-based climate interpretations are independent of potential processes controlling sediment deposition, which can be ambiguous. Lastly, climate interpretations from the MS record are based on the assumption that MS reflects the climate at the time material accumulated (Ellwood and Gose, 2006). A recent study questions this assumption, as dated leaf wax is variably older than the sediments from which it was recovered (Douglas et al., 2014). This indicates the possibility that the age of pedogenesis is likely older than the age of sediment deposition, and the age difference may be variable.

We propose a refinement of the Hall's Cave MS age model to enable more precise comparison with NBJ. Primarily, we include the top-most dates reported by Toomey (1993) that were not included in the age model of Ellwood and Gose (2006) (see Supplemental Material). The new age-model results in subtle differences to the MS time series (Fig. 7), although the youngest (<1 ka) part of the MS record is substantially affected by a hiatus in sedimentation delineated between stratigraphically overlapping but temporally distinct intervals. Furthermore, we plot abundance data of *Cryptotis* and *Notiosorex*, wet- and dry-adapted shrew species, respectively (Toomey, 1993), against time (using the same age-depth model discuss above) (Fig. 7) to provide additional context to the quantitative fauna data (i.e., variations in the relative proportion of the dry-adapted species) presented by Toomey et al. (1993) and used by Ellwood and Gose (2006) to provide a framework for interpreting MS variations.

The abundance data provide the same general understanding of Holocene climate gained from the proportion of the dry-adapted species, however, precision with respect to the timing and

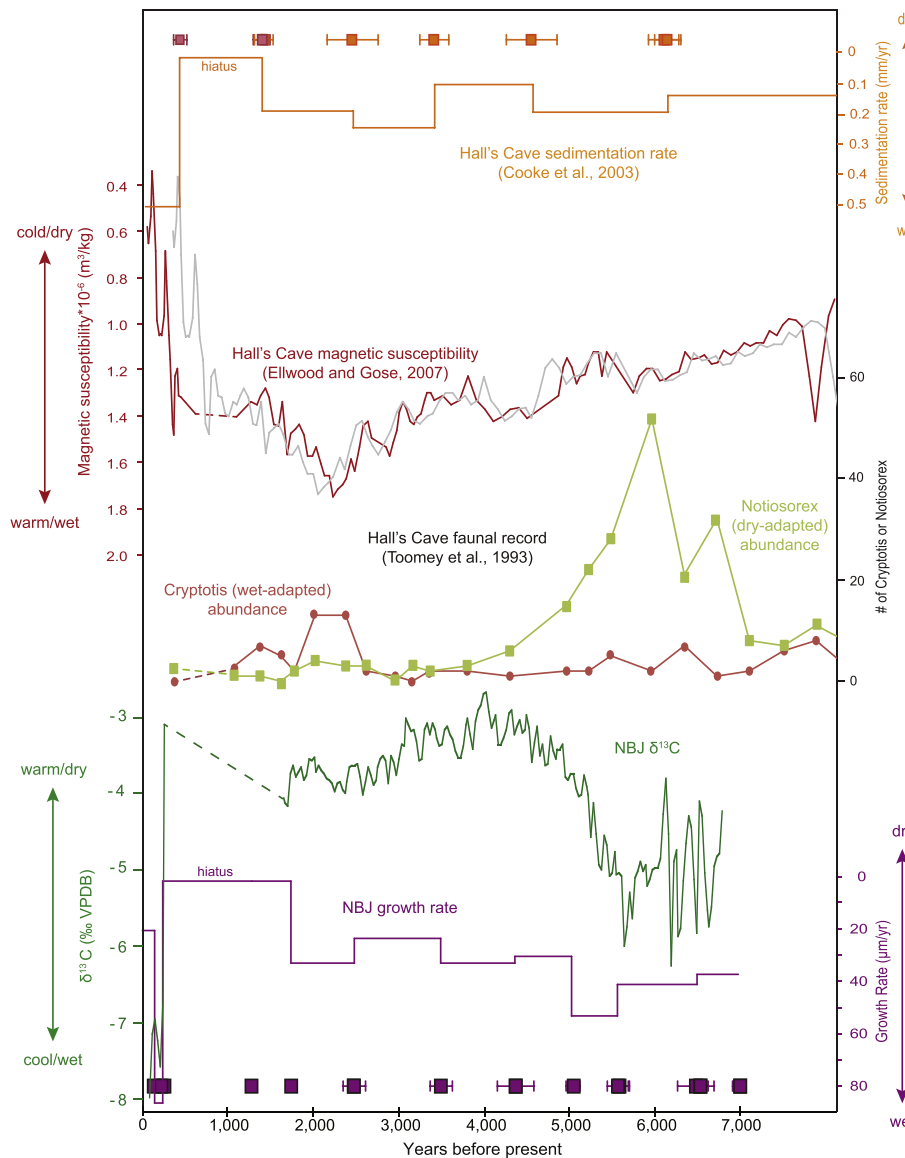


Fig. 7. Comparison of NBJ speleothem (Natural Bridge Caverns) growth rates (purple curve) and $\delta^{13}\text{C}$ values (dark green curve) to Hall's Cave faunal (light red and green), magnetic susceptibility (MS, red and gray), and sedimentation rate (orange). MS is plotted using the original (gray curve) and refined (dark red curve) age model, which are based on dates reported by Cooke et al. (2003) (orange squares) and Toomey et al. (1993) (dark red and orange squares), respectively. Sedimentation rate (orange curve) was calculated using these dates. Age constraints (U–Th) and uncertainty for speleothem NBJ are shown as purple squares (bottom). Note that axis is reversed for NBJ growth rate and Hall's Cave sedimentation rate and MS values.

magnitude of the variability is improved. For example, abundance of the dry-adapted species declined at ~5 ka, and remained low for the remainder of the Holocene (Fig. 7 and Supplemental Fig. 7). This timing is coincident with the establishment of present day soil conditions (Cooke et al., 2003) and the inferred threshold shift in vegetation. We note that small fluctuations in either the wet- or dry-adapted species resulted in large variation of the proportion of the dry-adapted species in the late Holocene (<4 ka) because the abundances of both species were so low (Supplemental Fig. 7). Interpretations of dry conditions based on the proportion of the dry-adapted species alone, therefore, results in the appearance of large magnitude shifts in moisture conditions that are not supported by the abundance data (Supplemental Fig. 7).

Both the MS record and speleothem $\delta^{13}\text{C}$ values suggest the culmination of warm conditions was followed by a return to cooler conditions in the late Holocene (Fig. 7). The timing of these variations, however, is offset between the two records. Maximum NBJ

$\delta^{13}\text{C}$ values occurred at 4 ka, whereas MS values peak at 2 ka. Furthermore, late Holocene MS and MS values reach their minimum at 2 ka and 1.5 ka, respectively. We note that the potential, variable age offsets between pedogenesis and deposition as cave sediment might account for such lags. Interestingly, the timing of the late Holocene increase in abundance of wet-adapted species (~2 ka) is similar to that of the minimum NBJ $\delta^{13}\text{C}$ values, which indicates the possibility that MS and faunal data from the same stratigraphic layer might reflect climate from different time intervals.

There are overlapping depositional hiatuses in both the Hall's Cave (1.0–0.5 ka) and NBJ (1.6–0.3 ka) records, suggesting the occurrence of the driest mid to late Holocene conditions during this time (Fig. 7). None of the NBJ speleothem proxies nor Hall's Cave MS record preserve anomalously dry mid Holocene conditions, despite evidence in other records from the region (including the Hall's Cave faunal record) (Figs. 6 and 7). Post-hiatus, the MS and NBJ records

preserve anomalous transitions in proxy values, but such transitions indicate opposing climate patterns. NBJ $\delta^{13}\text{C}$ values and trace-element concentrations both rapidly decreased from above average values to the lowest values preserved in the record (Fig. 4). The strong covariation between $\delta^{13}\text{C}$ values and trace-element concentrations, as well as the corresponding increase in speleothem growth rate, indicates that such variation was likely driven by a shift to wetter conditions. However, very few proxy records from in and near Texas, including tree ring records (Cleaveland et al., 2011), indicate anomalously wet conditions might have occurred within the last millennium. The MS record preserves anomalously low values, which indicates the occurrence of cold or dry conditions (Fig. 7). It is possible that post-hiatus MS values reflect the dry conditions that occurred during the depositional hiatus resulting from the age offset between pedogenesis (i.e., formation of magnetic minerals in the soil) and transport and deposition of sediment in the cave. This, however, is a tentative hypothesis as the nature of such offsets has yet to be studied. At this time, the anomalous post-hiatus variation in MS and speleothem growth rate, $\delta^{13}\text{C}$ values, and trace-element concentrations are poorly understood.

In summary, there is a general correspondence between mid to late Holocene climate trends reflected by NBJ and the Hall's Cave MS record. Both records indicate that (i) conditions warmed during the transition from the mid to late Holocene, (ii) there was a slight reprieve to cooler conditions ~2 ka, and (iii) driest conditions occurred ~1 ka resulting in a depositional hiatus in both records. The exact timing of these transitions is offset between the records, highlighting a need for additional well-dated, high-resolution climate reconstructions in the region to better constrain the timing of Holocene climate variation.

10. Paleoclimate data and model comparison

We consider the NBJ record in the context of existing, available paleoclimate model simulations. The Cooperative Holocene Mapping Project (COHMAP) consists of static, low-resolution (~4° latitude/longitude) simulations of key time intervals (e.g., 12 ka, 9 ka, 6 ka, and 0 ka) during the Holocene (Anderson et al., 1988). Whereas, higher resolution (2.7° latitude/longitude) static simulations of the mid Holocene (6 ka, referred to as 6K in modeling results) and preindustrial (PI; 1850) (Otto-Bliesner et al., 2006) and a transient simulation of the last deglaciation (21K; 21 to 0 ka) were completed using the Community Climate System Model (CCSM) (He, 2011). Details of the simulations and their applicability to Texas are discussed in [Supplemental Material](#). Overall, there is good agreement between proxy records (Fig. 6) and static paleoclimate simulations indicative of an overall pattern during the Holocene of warm and dry conditions relative to the wetter conditions preceding the Holocene (Fig. 8). Late Holocene climate variability that appears evident from proxy records, however, is not reflected in the transient simulation that spans the last 21,000 years (Fig. 9).

COHMAP results are broadly consistent with the existing compilation of proxy records from in and near Texas with (i) a warm, dry mid Holocene relative to present, and (ii) a drying trend across much of the Holocene. COHMAP was global in scope and coarse in resolution, however, relative to the present generation of global circulation models. Comparison of CCSM 6K and PI simulations indicates that the mid Holocene, relative to PI, had warmer, drier summers driven by enhanced seasonality and a decrease in GoM-derived moisture. Annual average 6K temperatures were not significantly different from PI in central Texas. Winter temperatures, however, were significantly lower (~1 to -1.5 °C) and summer temperatures were higher (1 °C) over central and northern Texas, consistent with the orbital configuration forcing enhanced seasonality (Otto-Bliesner et al., 2006) (Figs. 8a and b). Model

results indicate that the intensification of summer temperatures was stronger over the western U.S. and central and northern Great Plains than throughout much of Texas (Fig. 8b). Average annual precipitation was similar between 6K and PI simulations over much of Texas (Fig. 8c), but summer precipitation was greater over western Mexico and the southwestern U.S. and less over the southeastern U.S. (Fig. 8d). The former indicates that the North American Monsoon was likely stronger during the mid Holocene, which is consistent with warmer summers enhancing the land-ocean thermal gradient due to the low thermal inertia of land relative to ocean. The latter indicates that there was less southerly derived precipitation reaching the southern and northern Great Plains, which is consistent with the COHMAP model. The anti-phasing of moisture conditions over the southwestern U.S. and Great Plains is consistent with present day conditions, as described by Higgins et al. (1997), in which the onset of the North American Monsoon results in subsidence over the Great Plains, suppressing precipitation. Lastly, the model exhibits a bias toward westerly-derived precipitation relative to precipitation derived from the southeastern U.S. ([Supplemental Material](#)). Keeping in mind this bias, conditions in central Texas may have been drier in the mid Holocene than the model indicates. That is, decreased precipitation across the southeastern U.S. would have affected central Texas to a greater extent than the model indicates.

The transient model of the last deglaciation simulates a ~2 °C increase in mean annual temperature from 10 to 5 ka (Fig. 9). After 5 ka, mean annual temperatures are typically warmer than the early and mid Holocene, and there is no indication of a reprieve to cooler temperatures between 3 and 1 ka. From the early to late Holocene, summers cool and winters warm by ~3 and 4 °C, respectively. Simulated annual precipitation generally decreased from the end of the Pleistocene into the early Holocene with the most negative precipitation anomalies occurring ~9 to 7 ka (Fig. 9). During the first part of the Holocene, the decreasing trend in annual precipitation reflects a similar trend in fall and winter precipitation, whereas negative annual precipitation anomalies from 9 to 6 ka more closely resemble negative anomalies in spring and summer precipitation (Fig. 9). After 6 ka, positive and negative anomalies in annual precipitation occur evenly and consistently about the mean, and there is no prolonged interval of low annual precipitation during the late Holocene (Fig. 9). This is consistent with NBJ trace-element concentrations that indicate variable, but non-trending moisture conditions were likely from the mid to late Holocene. The seasonality of precipitation, however, changed beginning about 6 ka, as spring and summer precipitation increased and winter precipitation continued its downward pattern from the early Holocene.

Overall, the model simulations are consistent with proxy data indicating a warming pattern from the early to late Holocene. The transient simulation indicates temperatures progressively warmed until ~5 ka, after which temperatures plateaued, and driest conditions occurred between 9 and 7 ka (Fig. 9). These results indicate that peak warm and peak dry conditions were likely not coincident, which provides insight into the discrepancy among proxy records as to the timing of maximum warm and dry conditions. That is, proxies that are sensitive to both temperature and moisture conditions likely exhibit a range in the degree to which they are more or less sensitive to either temperature or moisture variability. Proxies more sensitive to moisture conditions may indicate an earlier occurrence of maximum warm/dry conditions, and vice versa. The lack of distinct climate variability in the transient simulation during the late Holocene is at odds with the proxy data, including the depositional hiatus in both the NBJ and Hall's Cave records. The discrepancy may reflect the tendency of more climate stability in models relative to proxy data (Collins et al., 2002;

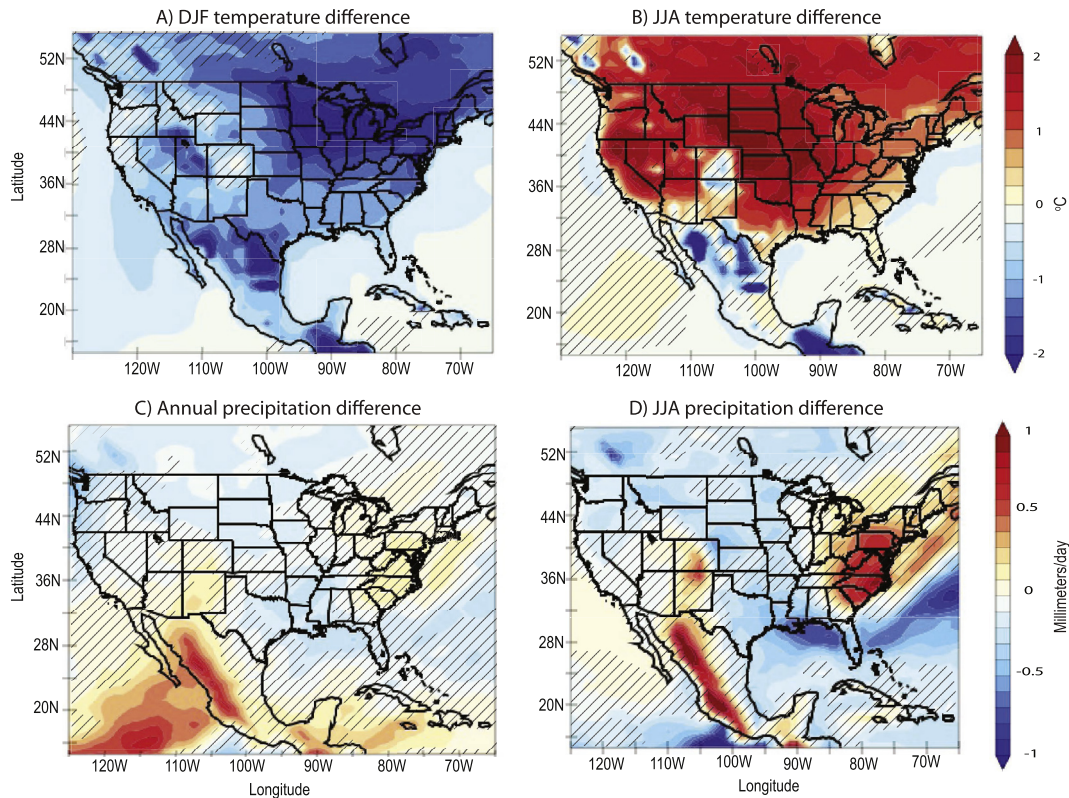


Fig. 8. Differences between 6K (6000 years before present) and PI (preindustrial) simulations for (A) winter (December, January, February; DJF) and (B) summer (June, July, August; JJA) surface temperature (°C), and (C) annual and (D) summer (JJA) precipitation (millimeters/day). Hashed areas are not statistically significant ($p > 0.05$) based on a Student's T-Test.

Goosse et al., 2005; Laepple and Huybers, 2014), or the absence of climate forcing influences, such as solar intensity variations and volcanic activity, in the simulation.

11. Speleothem $\delta^{18}\text{O}$ as a record of moisture-source variability

The NBJ $\delta^{18}\text{O}$ record does not exhibit strong correspondence with existing speleothem or GoM or east Pacific SSTs records from the broader region (e.g., Barron et al., 2003; Bernal et al., 2011; Doose et al., 1997; Hardt et al., 2010; Herbert, 2001; Kim et al., 2004; Poore et al., 2003, 2005, 2009; Richey et al., 2007, 2009, 2011; Prahl et al., 1995; Yamamoto et al., 2007) that would provide insight into potential climate processes governing speleothem $\delta^{18}\text{O}$ variability. However, NBJ $\delta^{18}\text{O}$ variability is similar to that of a proxy record of the relative strength of the Atlantic Meridional Overturning Circulation (AMOC; Thornalley et al., 2009). There is good visual correspondence from 5.5 to 1.5 ka between periodic variations in NBJ $\delta^{18}\text{O}$ values and the extent of water-column stratification of the inflow to a region of deep-water formation (Thornalley et al., 2009), and coherence between the two records is statistically significant (Fig. 10). Through low-latitude teleconnections, the strength of the AMOC affects the intensity of the Pacific storm track and the Aleutian Low, the latter of which influences the trajectory of the storm track over the western U.S. (e.g., Dima and Lohmann, 2007; Okumura et al., 2009; Vellinga and Wood, 2002; Wu et al., 2008). In simulations of an AMOC shutdown, cold anomalies in the North Atlantic translate over the narrow land corridor of Central America due to strong northeasterly trade winds that advect cold, dry air into the tropical eastern Pacific and promote evaporation (Wu et al., 2008). This drives the

southward shift of the Pacific Inter-tropical Convergence Zone, reduction of the meridional SST gradient, and perturbation of the Rossby waves that act to strengthen the Aleutian Low (Okumura et al., 2009). An enhanced Aleutian Low, coupled with intensified North Pacific High and high-pressure center over western Canada, results in greater NW–SE squeezing and steering of the storm track across western Canada (Oster et al., 2015). Additionally, enhancement of the Pacific meridional SST gradient drives the intensification of the jet stream (i.e., stronger winds) (e.g., Vellinga and Wood, 2002; Wu et al., 2008). Enhanced steering of an intensified storm track would drive greater contributions of Pacific-derived moisture to the southwestern U.S. (Asmerom et al., 2010; Feng et al., 2014a; Oster et al., 2015; Wagner et al., 2010). A stronger winter storm track would result in an increase of isotopically light, Pacific-derived moisture over Texas, consistent with depleted NBJ $\delta^{18}\text{O}$ values during intervals of weakened AMOC (Fig. 10).

The variability in NBJ $\delta^{18}\text{O}$ values is not coherent with that of speleothems from the eastern U.S. or southwestern Mexico. A composite speleothem record from West Virginia reflects variations in the seasonality of precipitation as controlled by the varying strength of the Bermuda High (Hardt et al., 2010). The record preserves a distinct shift ~4.2 ka, indicating an enhanced Bermuda High and greater summer moisture transport of GoM moisture to the site. The absence of such a shift in the NBJ record indicates that the proposed change in the intensity of the Bermuda High likely did not affect the Texas region, or that NBJ $\delta^{18}\text{O}$ variability is controlled by another process. NBJ $\delta^{18}\text{O}$ variability is also distinct from that of a speleothem from SW Mexico, which exhibits correspondence with $\delta^{18}\text{O}$ variability in PP1 from New Mexico through the Holocene until ~4.3 ka (Asmerom et al., 2007; Bernal et al., 2011). Dissimilarity between the SW Mexico and New Mexico records might be

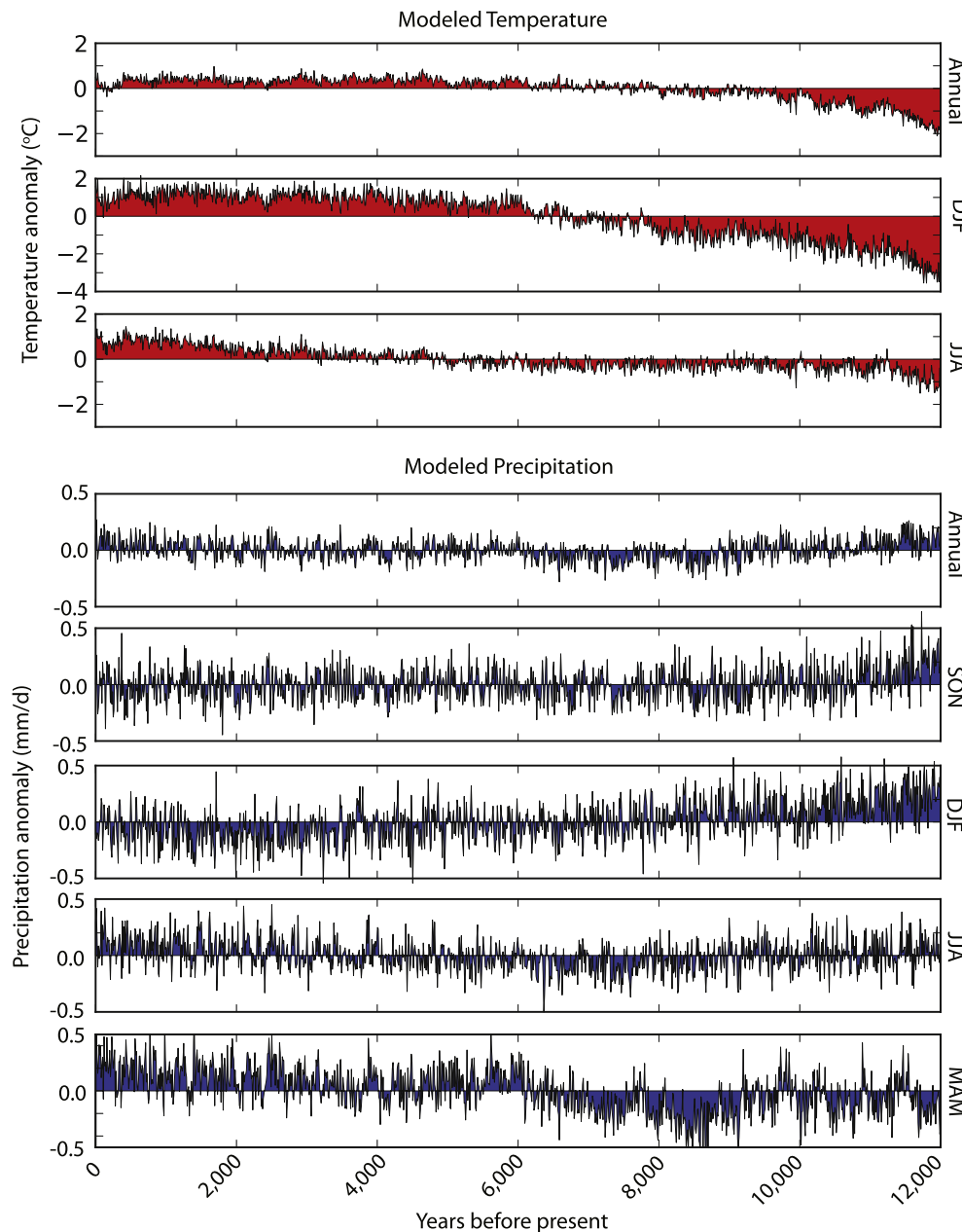


Fig. 9. Mean average and seasonal temperature and precipitation anomalies from Holocene average simulated by the 21K simulation for Texas (lat/long: 28.5–34 N, 94–103 W). SON = September, October, November. DJF = December, January, February. JJA = June, July, August. MAM = March, April, May.

related to a southward shift of the Inter-tropical Convergence Zone and increased El Niño frequency in the last ~5 to 4 ka (Bernal et al., 2011). Again, the lack of a distinct shift in the NBJ record between 5 and 4 ka indicates the influence of moisture transport processes was likely distinct from those influencing SW Mexico. Given the lack of correspondence between NBJ $\delta^{18}\text{O}$ values and those from other records in the broader region, it will be important to develop additional Texas speleothem records with overlapping age ranges.

12. Conclusions

A new speleothem (NBJ) reconstruction of Holocene climate represents a high resolution proxy record in the region, offering new insights into mid to late (7–0 ka) Holocene climate. NBJ trace-element concentration variations indicate that moisture conditions were variable but did not appear to increase or decrease during the

Holocene. The timing of a rapid transition from low to high NBJ $\delta^{13}\text{C}$ values is consistent with the establishment of present-day soil conditions by 5.0 ka (Cooke et al., 2003), which followed the progressive denudation of the landscape at a constant erosion rate during the last deglaciation (Cooke et al., 2003). We hypothesize that the shift in $\delta^{13}\text{C}$ values reflects a change in ecosystem composition and(or) productivity once a certain soil depth threshold was breached. Furthermore, such a change in the ecosystem overlying the cave could be responsible for the observed reduction in NBJ growth rate from the mid to late Holocene. This would indicate that speleothem growth might be a proxy for combined temperature-moisture conditions, rather than a direct moisture proxy. Lastly, NBJ $\delta^{18}\text{O}$ variability is decoupled from variations in trace-element concentrations, indicating a possible decoupling between moisture source and moisture amount over central Texas.

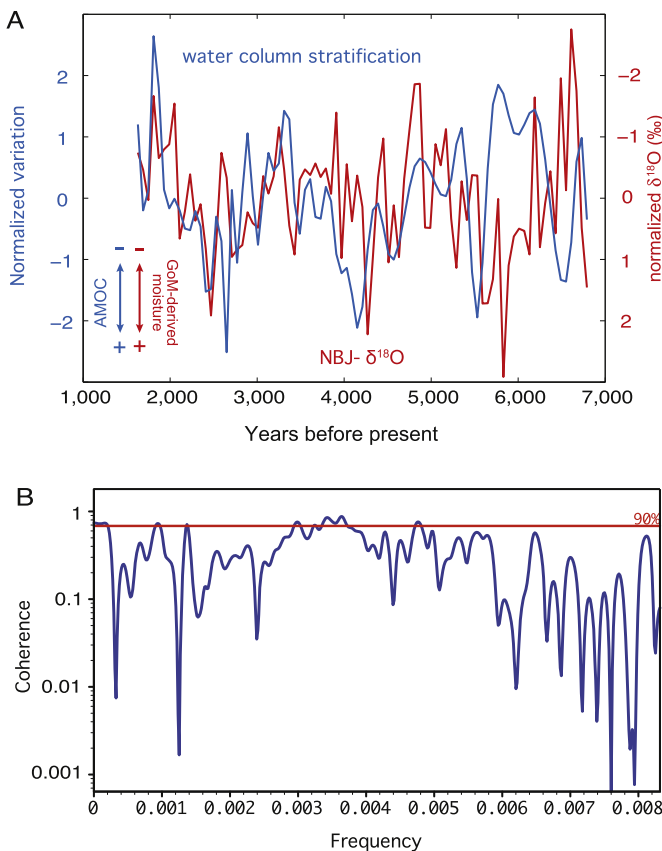


Fig. 10. A) Normalized variation in density differences between near surface and subthermocline marine waters in the North Atlantic (RAPiD-12-1K; Thornalley et al., 2009) (blue curve) and NBJ (Natural Bridge Caverns) speleothem $\delta^{18}\text{O}$ values (red curve). Greater stratification corresponds to enhanced freshwater flux to the North Atlantic and weaker AMOC. NBJ values are plotted inversely. Both data sets are interpolated to 60 year intervals, the average sampling resolution of RAPiD-12-1K. B) Multi-taper method (MTM) coherence analysis (Ghil et al., 2000) between interpolated NBJ and RAPiD-12-1K records. Red line marks the 90% confidence interval.

NBJ $\delta^{13}\text{C}$ values are consistent with other records of mid to late Holocene climate from in and near Texas that indicate (i) a warming/drying trend from early to mid Holocene, (ii) a brief shift away from warm/dry conditions in the transition from the mid to late Holocene, and (iii) a dry interval in the late Holocene. The absence of either an upward or downward pattern in NBJ trace-element concentrations, which are a proxy for moisture conditions, indicate that $\delta^{13}\text{C}$ variability might dominantly reflect temperature rather than moisture. $\delta^{18}\text{O}$ variability corresponds poorly with nearby speleothem records and GoM and Pacific SSTs, but is coherent with a reconstruction of AMOC from the North Atlantic. The strength and trajectory of the Pacific winter storm track is responsive to variations in AMOC strength and influences the proportion of Pacific-vs. Gulf of Mexico-derived moisture reaching Texas as reflected by speleothem $\delta^{18}\text{O}$ values.

Acknowledgments

We thank the Natural Bridge Caverns for access. Research was supported by the Environmental Science Institute, Jackson School of Geosciences, NSF P2C2 Program (ATM-0823665), EPA's STAR Fellowship Program (FP917114), California Presidential Post-doctoral Fellowship, and Philanthropic Educational Organization. Any use of trade, firm, or product names is for descriptive purposes only and does not imply endorsement by the U.S. Government. This

manuscript benefitted from suggestions from Benjamin F. Hardt and two anonymous reviewers.

Appendix A. Supplementary data

Supplementary data related to this article can be found at <http://dx.doi.org/10.1016/j.quascirev.2015.06.023>.

References

- Anderson, P.M., Barnosky, C.W., Bartlein, P.J., Behl, P., Brubaker, L., Cushing, E.J., Dodson, J., Dvoretsky, B., Guetter, P.J., Harrison, S.P., Huntley, B., Kutzback, J.E., Markgraf, V., Marvel, R., McGlone, M.S., Mix, A., Moar, N.T., Morley, J., Perrott, R.A., Peterson, G.M., Prell, W.L., Prentice, I.C., Ritchie, J.C., Roberts, N., Ruddiman, W.F., Salinger, M.J., Spaulding, W.G., Street-Perrott, F.A., Thompson, R.S., Wang, P.K., Webb III, T., Winkler, M.G., Wright Jr., H.E., 1988. Climatic changes of the last 18,000 years: observations and model simulations. *Science* 241, 1043–1052.
- Asmerom, Y., Polyak, V., Burns, S., Rasmussen, J., 2007. Solar forcing of Holocene climate: new insights from a speleothem record, southwestern United States. *Geology* 35, 1. <http://dx.doi.org/10.1130/G22865A.1>.
- Asmerom, Y., Polyak, V.J., Burns, S.J., 2010. Variable winter moisture in the southwestern United States linked to rapid glacial climate shifts. *Nat. Geosci.* 3, 114–117. <http://dx.doi.org/10.1038/NGEO754>.
- Ault, T.R., Cole, J.E., Overpeck, J.T., Pederson, G.T., St George, S., Otto-Btiesner, B., Woodhouse, C.A., Deser, C., 2013. The continuum of hydroclimate variability in western North America during the last millennium. *J. Clim.* 26, 5863–5878. <http://dx.doi.org/10.1175/JCLI-D-11-00732.1>.
- Austin American-Statesman, 201117 Oct 2011. Billions in Losses, the Drought in Texas: A Multiday Series. Austin-American Statesman, p. A1.
- Baker, A., Barnes, W.L., Smart, P.L., 1997. Variations in the discharge and organic matter content of stalagmite drip waters in Lower Cave. *Bristol. Hydrol. Process* 11, 1541–1555.
- Baldini, J.U., 2010. Cave Atmosphere Controls on Stalagmite Growth Rate and Palaeoclimate Records. In: *Geol. Soc. London, Spec. Publ.* 336, pp. 283–294. <http://dx.doi.org/10.1144/SP336.15>.
- Banner, J.L., Guilfoyle, A., James, E.W., Stern, L.A., Musgrave, M., 2007. Seasonal variations in modern speleothem calcite growth in central Texas, U.S.A. *J. Sediment. Res.* 77, 615–622.
- Bar-Matthews, M., Ayalon, A., Kaufman, A., Wasserburg, G.J., 1999. The Eastern Mediterranean paleoclimate as a reflection of regional events: Soreq cave, Israel. *Earth Planet. Sci. Lett.* 166, 85–95.
- Barron, J.A., Heusser, L., Herbert, T., Lyle, M., 2003. High-resolution climatic evolution of coastal northern California during the past 16,000 years. *Paleoceanography* 18, 1020. <http://dx.doi.org/10.1029/2002PA000768>.
- Berkelhammer, M., Stott, L., Yoshimura, K., Johnson, K., Sinha, A., 2011. Synoptic and mesoscale controls on the isotopic composition of precipitation in the western United States. *Clim. Dyn.* 38, 433–454. <http://dx.doi.org/10.1007/s00382-011-1262-3>.
- Bernal, J.P., Lachniet, M., McCulloch, M., Mortimer, G., Morales, P., Cienfuegos, E., 2011. A speleothem record of Holocene climate variability from southwestern Mexico. *Quat. Res.* 75, 104–113. <http://dx.doi.org/10.1016/j.yqres.2010.09.002>.
- Blum, M.D., Toomey III, R.S., Valastro Jr., S., 1994. Fluvial response to Late Quaternary climatic and environmental change, Edwards Plateau, Texas. *Palaeogeogr. Palaeoclimatol. Palaeoecol.* 108, 1–21.
- Bousman, C.B., 1998. Palaeoenvironmental change in central Texas: the palynological evidence. *Plains Anthropol.* 2, 201–219.
- Boulter, C., Bateman, M.D., Frederick, C.D., 2010. Understanding geomorphic responses to environmental change: a 19 000-year case study from semi-arid central Texas, USA. *J. Quat. Sci.* 25, 889–902. <http://dx.doi.org/10.1002/jqs.1365>.
- Breecker, D.O., Payne, A.E., Quade, J., Banner, J.L., Ball, C.E., Meyer, K.W., Cowan, B.D., 2012. The sources and sinks of CO₂ in caves under mixed woodland and grassland vegetation. *Geochim. Cosmochim. Acta* 96, 230–246. <http://dx.doi.org/10.1016/j.gca.2012.08.023>.
- Bryant Jr., V.M., 1977. A 16,000 year pollen record of vegetational change in central Texas. *Palynology* 1, 143–156.
- Buck, B.J., Monger, H.C., 1999. Stable isotopes and soil-geomorphology as indicators of Holocene climate change, northern Chihuahuan Desert. *J. Arid Environ.* 43, 357–373. <http://dx.doi.org/10.1006/jare.1999.0584>.
- Casteel, R.C., Banner, J.L., 2015. Temperature-driven seasonal calcite growth and drip water trace element variations in a well-ventilated Texas cave: implications for speleothem paleoclimate studies. *Chem. Geol.* 392, 43–58. <http://dx.doi.org/10.1016/j.chemgeo.2014.11.002>.
- Cheng, H., Edwards, R.L., Hoff, J., Gallup, C.D., Richards, D.A., Asmerom, Y., 2000. The half-lives of uranium-234 and thorium-230. *Chem. Geol.* 169, 17–33.
- Cleaveland, M.K., Votteler, T.H., Stahle, D.K., Casteel, R.C., Banner, J.L., 2011. Extended chronology of drought in south, central, southeastern, and west Texas. *Tex. Water J.* 2, 54–96.
- Collins, M., Osborn, T.J., Tett, S.F.B., Briffa, K.R., Schweingruber, F.H., 2002. A comparison of the variability of a climate model with paleotemperature estimates from a network of tree-ring densities. *J. Clim.* 15, 1497–1515.

- Cooke, M.J., Stern, L.A., Banner, J.L., Mack, L.E., Stafford, T.W., Toomey, R.S., 2003. Precise timing and rate of massive late Quaternary soil denudation. *Geology* 31, 853–856. <http://dx.doi.org/10.1130/G19749.1>.
- Cooke, M.J., Stern, L.A., Banner, J.L., Mack, L.E., 2007. Evidence for the silicate source of relict soils on the Edwards Plateau, central Texas. *Quatern. Res.* 67, 275–285.
- Cordova, C.E., Johnson, W.C., Mandel, R.D., Palmer, M.W., 2011. Late Quaternary environmental change inferred from phytoliths and other soil-related proxies: case studies from the central and southern Great Plains, USA. *Catena* 85, 87–108. <http://dx.doi.org/10.1016/j.catena.2010.08.015>.
- Cruz, F.W., Burns, S.J., Jercinovic, M., Karmann, I., Sharp, W.D., Vuille, M., 2007. Evidence of rainfall variations in Southern Brazil from trace element ratios (Mg/Ca and Sr/Ca) in a Late Pleistocene stalagmite. *Geochim. Cosmochim. Acta* 71, 2250–2263. <http://dx.doi.org/10.1016/j.gca.2007.02.005>.
- Denniston, R.F., DuPree, M., Dorale, J.A., Asmerom, Y., Polyak, V.J., Carpenter, S.J., 2007. Episodes of late Holocene aridity recorded by stalagmites from Devil's Icebox Cave, central Missouri, USA. *Quat. Res.* 68, 45–52.
- Dima, M., Lohmann, G., 2007. A hemispheric mechanism for the Atlantic Multi-decadal Oscillation. *J. Clim.* 20, 2706–2719. <http://dx.doi.org/10.1175/JCLI4174.1>.
- Dirmeyer, P.A., Brubaker, K.L., 2007. Characterization of the global hydrologic cycle from a back-trajectory analysis of atmospheric water vapor. *J. Hydrometeorol.* 8, 20–37. <http://dx.doi.org/10.1175/JHM557.1>.
- Dong, B., Sutton, R.T., 2007. Enhancement of ENSO variability by a weakened Atlantic Thermohaline circulation in a coupled GCM. *J. Clim.* 20, 4920–4939. <http://dx.doi.org/10.1175/JCLI4284.1>.
- Dong, B., Sutton, R.T., Scaife, A.A., 2006. Multidecadal modulation of El Niño–Southern Oscillation (ENSO) variance by Atlantic Ocean sea surface temperatures. *Geophys. Res. Lett.* 33, L08705. <http://dx.doi.org/10.1029/2006GL025766>.
- Doose, H., Prahl, F.G., Lyle, M.W., 1997. Biomarker temperature estimates for modern and last glacial surface waters of the California Current System between 33° and 42°N. *Paleoceanography* 12, 615–622. <http://dx.doi.org/10.1029/97PA00821>.
- Dorale, J.A., Edwards, R.L., Ito, E., Gonzalez, L.A., 1998. Climate and vegetation history of the midcontinent from 75 to 25 ka: a speleothem record from crevice cave, Missouri, USA. *Science* 282, 1871–1874.
- Douglas, P.M.J., Pagani, M., Eglinton, T.I., Brenner, M., Hodell, D.A., Curtis, J.H., Ma, K.F., Breckenridge, A., 2014. Pre-aged plant waxes in tropical lake sediments and their influence on the chronology of molecular paleoclimate proxy records. *Geochim. Cosmochim. Acta* 141, 346–364. <http://dx.doi.org/10.1016/j.gca.2014.06.030>.
- Dreybrodt, W., 1999. Chemical kinetics, speleothem growth and climate. *Boreas* 28, 347–356. <http://dx.doi.org/10.1080/030094899422073>.
- Edwards, R., Chen, J.H., Wasserburg, G.J., 1987. ^{238}U – ^{234}U – ^{230}Th – ^{232}Th systematics and the precise measurement of time over the past 500,000 years. *Earth Planet. Sci. Lett.* 81, 175–192.
- Edwards, R.L., Beck, J.W., Burr, G.S., Donahue, D.J., Chappell, J.M.A., Bloom, A.L., Druffel, E.R.M., Taylor, F.W., 1993. A large drop in atmospheric ^{14}C / ^{12}C and reduced melting in the Younger Dryas, documented with ^{230}Th ages of corals. *Science* 260, 962–968.
- Ellwood, B.B., Gose, W.A., 2006. Heinrich H1 and 8200 yr B.P. climate events recorded in Hall's Cave, Texas. *Geology* 34, 753–756. <http://dx.doi.org/10.1130/G22549.1>.
- Elliot, W.R., Veni, G., 1994. The Caves and Karst of Texas – 1994 NSS Convention Guidebook.
- Fairchild, I.J., Borsato, A., Tooth, A.F., Frisia, S., Hawkesworth, C.J., Huang, Y.M., McDermott, F., Spiro, B., 2000. Controls on trace element (Sr-Mg) compositions of carbonatic cave waters: implications for speleothem climatic records. *Chem. Geol.* 166, 255–269.
- Fairchild, I.J., Smith, C.L., Baker, A., Fuller, L., Spotl, C., Matthey, D., McDermott, F., E.I.M.F., 2006. Modification and preservation of environmental signals in speleothems. *Earth Sci. Rev.* 75, 105–153.
- Fairchild, I.J., Treble, P.C., 2009. Trace elements in speleothems as recorders of environmental change. *Quat. Sci. Rev.* 28, 449–468. <http://dx.doi.org/10.1016/j.quascirev.2008.11.007>.
- Feng, S., Hu, Q., Oglesby, R.J., 2010. Influence of Atlantic sea surface temperatures on persistent drought in North America. *Clim. Dyn.* 37, 569–586. <http://dx.doi.org/10.1007/s00382-010-0835-x>.
- Feng, W., Casteel, R.C., Banner, J.L., Heinze-Fry, A., 2014a. Oxygen isotope variations in rainfall, drip-water and speleothem calcite from a well-ventilated cave in Texas, USA: assessing a new speleothem temperature proxy. *Geochim. Cosmochim. Acta* 127, 233–250. <http://dx.doi.org/10.1016/j.gca.2013.11.039>.
- Feng, W., Hardt, B.F., Banner, J.L., Meyer, K.J., James, E.W., Musgrove, M., Edwards, R.L., Cheng, H., Min, A., 2014a. Changing amounts and sources of moisture in the U.S. southwest since the Last Glacial maximum in response to global climate change. *Earth Planet. Sci. Lett.* 401, 47–56. <http://dx.doi.org/10.1016/j.epsl.2014.05.046>.
- Ferring, C.R., 1990. Late Quaternary geology and geoarchaeology of the Upper Trinity River drainage basin, Texas. In: Guidebook for Geological Society of America Fieldtrip, 11. Dallas Geological Society, pp. 1–81.
- Genty, D., Baker, A., Massault, M., Proctor, C., Gilmour, M., Pons-Branchu, E., Hamelin, B., 2001. Dead carbon in stalagmites: carbonate bedrock paleodissolution vs. ageing of soil organic matter. Implications for ^{13}C variations in speleothems. *Geochim. Cosmochim. Acta* 65, 3443–3457.
- Genty, D., Blamart, D., Ouahdi, R., Gilmour, M., Baker, A., Jouzel van Exter, S., 2003. Precise dating of Dansgaard-Oeschger climate oscillations in western Europe from stalagmite data. *Nature* 421, 833–837.
- Gershunov, A., Barnett, T.P., 1998. Inter-decadal modulation of ENSO teleconnections. *Bull. Am. Meteorol. Soc.* 79, 2715–2725.
- Ghil, M., Allen, R.M., Dettinger, M.D., Ide, K., Kondrashov, D., Mann, M.E., Robertson, A., Saunders, A., Tian, Y., Varadi, F., Yiou, P., 2000. Advanced spectral methods for climatic time series. *Rev. Geophys.* 40, 3.1–3.41. <http://dx.doi.org/10.1029/2000GR000092>.
- Gimeno, L., Stohl, A., Trigo, R., 2012. Oceanic and terrestrial sources of continental precipitation. *Rev. Geophys.* 50, 1–41. <http://dx.doi.org/10.1029/2012RG000389>.
- Goodfriend, G.A., Ellis, G.L., 2000. Stable carbon isotope record of middle to late Holocene climate changes from land snail shells at Hinds Cave, Texas. *Quat. Int.* 67, 47–60. [http://dx.doi.org/10.1016/S1040-6182\(00\)00008-2](http://dx.doi.org/10.1016/S1040-6182(00)00008-2).
- Goosse, H., Renessen, H., Timmermann, A., Bradley, R.S., 2005. Internal and forced climate variability during the last millennium: a model-data comparison using ensemble simulations. *Quat. Sci. Rev.* 24, 1345–1360. <http://dx.doi.org/10.1016/j.quascirev.2004.12.009>.
- Hall, S.A., 1990. Channel trenching and climatic change in the southern U.S. Great Plains. *Geology* 18, 342–345.
- Hall, S.A., Boutton, T.W., Lintz, C.R., Baugh, T.G., 2012. New correlation of stable carbon isotopes with changing late-Holocene fluvial environments in the Trinity River basin of Texas, USA. *Holocene* 22, 541–549. <http://dx.doi.org/10.1177/0959683611427338>.
- Hardt, B., Rowe, H., Springer, G., Cheng, H., Edwards, R.L., 2010. The seasonality of east central North American precipitation based on three coeval Holocene speleothems from southern West Virginia. *Earth Planet. Sci. Lett.* 295, 342–348. <http://dx.doi.org/10.1016/j.epsl.2010.04.002>.
- He, F., 2011. Simulating Transient Climate Evolution of the Last Deglaciation with CCSM3. University of Wisconsin-Madison (PhD Dissertation).
- Hellstrom, J., McCulloch, M., Stone, J., 1998. A detailed 31,000-year record of climate and vegetation change, from the isotope geochemistry of two New Zealand speleothems. *Quat. Res.* 50, 167–178.
- Herbert, T.D., 2001. Collapse of the California Current during glacial maxima linked to climate change on land. *Science* 293, 71–76. <http://dx.doi.org/10.1126/science.1059209>.
- Higgins, R.W., 1997. Influence of the North American Monsoon System on the U.S. summer precipitation regime. *J. Clim.* 10, 2600–2622.
- Higgins, R.W., Yao, Y., Yarosh, E.S., Janowiak, J.E., Mo, K.C., 1997. Influence of the Great Plains Low-Level Jet on summertime precipitation and moisture transport over the Central United States. *J. Clim.* 10, 481–507.
- Holliday, V.T., 2001. Stratigraphy and geochronology of upper Quaternary eolian sand on the Southern High Plains of Texas and New Mexico, United States. *Geol. Soc. Am. Bull.* 113, 88–108.
- Holliday, V.T., Mayer, J.H., Fredlund, G.G., 2008. Late Quaternary sedimentology and geochronology of small playas on the Southern High Plains, Texas and New Mexico, U.S.A. *Quat. Res.* 70, 11–25. <http://dx.doi.org/10.1016/j.yqres.2008.02.009>.
- Holmgren, C.A., Norris, J., Betancourt, J.L., 2007. Inferences about winter temperatures and summer rains from the late Quaternary record of C_4 perennial grasses and C_3 desert shrubs in the northern Chihuahuan Desert. *J. Quat. Sci.* 22, 141–161. <http://dx.doi.org/10.1002/j.qs.1023>.
- Holmgren, C.A., Peñalba, M.C., Rylander, K.A., Betancourt, J.L., 2003. A 16,000 ^{14}C yr B.P. packrat midden series from the USA-Mexico Borderlands. *Quat. Res.* 60, 319–329. <http://dx.doi.org/10.1016/j.yqres.2003.08.001>.
- Hu, Q., Feng, S., 2001a. Variations of teleconnection of ENSO and interannual variation in summer rainfall in the central United States. *J. Clim.* 14, 2469–2481.
- Hu, Q., Feng, S., 2001b. Climatic role of the southerly flow from the Gulf of Mexico in interannual variations in summer rainfall in the Central United States. *J. Clim.* 14, 3156–3171.
- Hu, Q., Feng, S., Oglesby, R.J., 2011. Variations in North American summer precipitation driven by the Atlantic multidecadal oscillation. *J. Clim.* 24, 5555–5570. <http://dx.doi.org/10.1175/2011JCLI4060.1>.
- Humphrey, J.D., Ferring, C.R., 1994. Stable isotopic evidence for latest Pleistocene and Holocene climatic change in north-central Texas. *Quat. Res.* 41, 200–213. <http://dx.doi.org/10.1006/qres.1994.1022>.
- Johnson, K.R., Hu, C.Y., Belshaw, N.S., Henderson, G.M., 2006. Seasonal trace-element and stable-isotope variations in a Chinese speleothem: the potential for high-resolution paleomonsoon reconstruction. *Earth Planet. Sci. Lett.* 244, 394–407.
- Karmann, I., Cruzir, F., Vianajr, O., Burns, S., 2007. Climate influence on geochemistry parameters of waters from Santana–Pérolas cave system, Brazil. *Chem. Geol.* 244, 232–247. <http://dx.doi.org/10.1016/j.chemgeo.2007.06.029>.
- Kim, J.-H., Rimbu, N., Lorenz, S.J., Lohmann, G., Nam, S.-I., Schouten, S., Rühlemann, C., Schneider, R.R., 2004. North Pacific and North Atlantic sea-surface temperature variability during the Holocene. *Quat. Sci. Rev.* 23, 2141–2154. <http://dx.doi.org/10.1016/j.quascirev.2004.08.010>.
- Koster, R.D., Dirmeyer, P., Guo, Z., Bonan, G., 2004. Regions of strong coupling between soil moisture and precipitation. *Science* 305, 1138–1140.
- Laepple, T., Huybers, P., 2014. Ocean surface temperature variability: large model–data differences at decadal and longer periods. *Proc. Natl. Acad. Sci.* 111, 16682–16687. <http://dx.doi.org/10.1073/pnas.1412077111>.
- Larkin, T.J., Bomar, G.W., 1983. Climatic Atlas of Texas. Texas Department of Water Resources, Austin.
- Mann, M.E., Zhang, Z., Rutherford, S., Bradley, R.S., Hughes, M.K., Shindell, D., Ammann, C., Faluvegi, G., Ni, F., 2009. Global signatures and dynamical origins of the Little Ice Age and Medieval Climate Anomaly. *Science* 326, 1256–1260. <http://dx.doi.org/10.1126/science.1177303>.

- Marcott, S.A., Shakun, J.D., Clark, P.U., Mix, A.C., 2013. A reconstruction of regional and global temperature for the past 11,300 years. *Science* 339, 1198–1201. <http://dx.doi.org/10.1126/science.1228026>.
- Mattey, D.P., Fairchild, I.J., Atkinson, T.C., Latin, J.-P., Ainsworth, M., Durell, R., 2010. Seasonal Microclimate Control of Calcite Fabrics, Stable Isotopes and Trace Elements in Modern Speleothem from St Michaels Cave, Gibraltar. In: *Geol. Soc. London, Spec. Publ.* 336, pp. 323–344. <http://dx.doi.org/10.1144/SP336.17>.
- McCabe, G.J., Betancourt, J.L., Gray, S.T., Palecki, M. a, Hidalgo, H.G., 2008. Associations of multi-decadal sea-surface temperature variability with US drought. *Quat. Int.* 188, 31–40. <http://dx.doi.org/10.1016/j.quaint.2007.07.001>.
- McCabe, G.J., Palecki, M.A., Betancourt, J.L., 2004. Pacific and Atlantic Ocean influences on multidecadal drought frequency in the United States. *Proc. Natl. Acad. Sci. U.S.A.* 101, 4136–4141.
- McDonald, J., Drysdale, R., Hill, D., Chisari, R., Wong, H., 2007. The hydrochemical response of cave drip waters to sub-annual and inter-annual climate variability, Wombeyan Caves, SE Australia. *Chem. Geol.* 244, 605–623.
- Meier, H.A., Driese, S.g., Nordt, L.C., Forman, S.L., Dworkin, S.I., 2014. Interpretation of Late Quaternary climate and landscape variability based upon buried soil macro- and micromorphology, geochemistry, and stable isotopes of soil organic matter, Owl Creek, central Texas, USA. *Catena* 114, 157–168. <http://dx.doi.org/10.1016/j.catena.2013.08.019>.
- Meyer, K.W., Feng, W., Breecker, D.O., Banner, J.L., Guilfoyle, A., 2014. Interpretation of speleothem calcite $\delta^{13}\text{C}$ variations: evidence from monitoring soil CO_2 , drip water, and modern speleothem calcite in central Texas. *Geochim. Cosmochim. Acta* 142, 281–298. <http://dx.doi.org/10.1016/j.gca.2014.07.027>.
- Mickler, P.J., Banner, J.L., Stern, L., Asmerom, Y., Edwards, R.L., Ito, E., 2004. Stable isotope variations in modern tropical speleothems: evaluating equilibrium vs. kinetic isotope effects. *Geochim. Cosmochim. Acta* 68, 4381–4393. <http://dx.doi.org/10.1016/j.gca.2004.02.012>.
- Mickler, P.J., Stern, L.A., Banner, J.L., 2006. Large kinetic isotope effects in modern speleothems. *Geol. Soc. Am. Bull.* 118, 65–81. <http://dx.doi.org/10.1130/B25698.1>.
- Musgrove, M., Banner, J.L., 2004. Controls on the spatial and temporal variability of vadose dripwater geochemistry: Edwards aquifer, central Texas1. *Geochim. Cosmochim. Acta* 68, 1007–1020. <http://dx.doi.org/10.1016/j.gca.2003.08.014>.
- Musgrove, M., Banner, J.L., Mack, L.E., Combs, D.M., James, E.W., Edwards, R.L., 2001. Geochronology of late Pleistocene to Holocene speleothems from central Texas: Implications for regional paleoclimate. *Geol. Soc. Am. Bull.* 113, 1532–1543.
- Myoung, B., Nielsen-Gammon, J.W., 2010. The convective instability pathway to warm season drought in Texas. Part I: the role of convective inhibition and its modulation by soil moisture. *J. Clim.* 23, 4461–4473. <http://dx.doi.org/10.1175/2010JCLI2946.1>.
- Nordt, L.C., Boutton, T.W., Hallmark, C.T., Water, M.R., 1994. Late Quaternary vegetation and climate changes in central Texas based on the isotopic composition of organic carbon. *Quatern. Res.* 41, 109–120. <http://dx.doi.org/10.1006/qres.1994.1012>.
- Nordt, L.C., Boutton, T.W., Jacob, J.S., Mandel, R.D., 2002. C_4 plant productivity and climate- CO_2 variations in south-central Texas during the late Quaternary. *Quat. Res.* 58, 182–188. <http://dx.doi.org/10.1006/qres.2002.2344>.
- Nordt, L., von Fischer, J., Tieszen, L., 2007. Late Quaternary temperature record from buried soils of the North American Great Plains. *Geology* 35, 159–162. <http://dx.doi.org/10.1130/G23345A.1>.
- Okumura, Y.M., Deser, C., Hu, A., Timmermann, A., Xie, S.-P., 2009. North Pacific climate response to freshwater forcing in the Subarctic North Atlantic: oceanic and atmospheric pathways. *J. Clim.* 22, 1424–1445. <http://dx.doi.org/10.1175/2008JCLI2511.1>.
- Oster, J.L., Montañez, I.P., Sharp, W.D., Cooper, K.M., 2009. Late Pleistocene California droughts during deglaciation and Arctic warming. *Earth Planet. Sci. Lett.* 288, 434–443.
- Oster, J.L., Montañez, I.P., Guilderson, T.P., Sharp, W.D., Banner, J.L., 2010. Modeling speleothem $\delta^{13}\text{C}$ variability in a Central Sierra Nevada cave using ^{14}C and $^{87}\text{Sr}/^{86}\text{Sr}$. *Geochim. Cosmochim. Acta* 74, 5228–5242.
- Oster, J.L., Montañez, I.P., Kelley, N.P., 2012. Response of a modern cave system to large seasonal precipitation variability. *Geochim. Cosmochim. Acta* 91, 92–108. <http://dx.doi.org/10.1016/j.gca.2012.05.027>.
- Oster, J.L., Ibarra, D.E., Winnick, M.J., Maher, K., 2015. Steering of westerly storms over western North America at the Last Glacial Maximum. *Nat. Geosci.* 8, 1–5. <http://dx.doi.org/10.1038/NGEO2365>.
- Otto-Bliesner, B.L., Brady, E.C., Clauzet, G., Tomas, R., Levis, S., Kothavala, Z., 2006. Last glacial maximum and holocene climate in CCSM3. *J. Clim.* 19, 2526–2544. <http://dx.doi.org/10.1175/JCLI3748.1>.
- Pape, J.R., Banner, J.L., Mack, L.E., Musgrove, M., Guilfoyle, A., 2010. Controls on oxygen isotope variability in precipitation and cave drip waters, central Texas, USA. *J. Hydrol.* 385, 203–215. <http://dx.doi.org/10.1016/j.jhydrol.2010.02.021>.
- Partin, J.W., Quinn, T.M., Shen, C.-C., Emile-Geay, J., Taylor, F.W., Maupin, C.R., Lin, K., Jackson, C.S., Banner, J.L., Sinclair, D.J., Huh, C., 2013. Multidecadal rainfall variability in South Pacific Convergence Zone as revealed by stalagmite geochemistry. *Geology* 41, 1143–1146. <http://dx.doi.org/10.1130/G34718.1>.
- Paton, C., Hellstrom, J., Bence, P., Woodhead, J., Hergt, J., 2011. Iolite: Freeware for the visualization and processing of mass spectrometric data. *J. Anal. A. T. Spectrom.* 26, 2508–2518.
- Polyak, V.J., Cokendolpher, J.C., Norton, R.A., Asmerom, Y., 2001. Wetter and cooler late Holocene climate in the southwestern United States from mites preserved in stalagmites. *Geology* 29, 643–646.
- Polyak, V.J., Asmerom, Y., 2001. Late Holocene climate and cultural changes in the southwestern United States. *Science* 294, 148–151. <http://dx.doi.org/10.1126/science.1062771>.
- Polyak, V.J., Rasmussen, J.B.T., Asmerom, Y., 2004. Prolonged wet period in the southwestern United States through the Younger Dryas. *Geology* 32, 5–8. <http://dx.doi.org/10.1130/G19957.1>.
- Poore, R.Z., Delong, K.L., Richey, J.N., Quinn, T.M., 2009. Evidence of multidecadal climate variability and the Atlantic Multidecadal Oscillation from a Gulf of Mexico sea-surface temperature-proxy record. *Geo Mar Lett.* 29, 477–484.
- Poore, R.Z., Dowsett, H.J., Verardo, S., Quinn, T.M., 2003. Millennial- to century-scale variability in Gulf of Mexico Holocene climate records. *Paleoceanography* 18, 1048. <http://dx.doi.org/10.1029/2002PA000868>.
- Poore, R.Z., Pavich, M.J., Grissino-Mayer, H.D., 2005. Record of the North American southwest monsoon from Gulf of Mexico sediment cores. *Geology* 33, 209–212.
- Prahl, G., Pisias, N., Sparrow, M.A., Sabin, A., 1995. Assessment of sea-surface temperature at 42° N in the California Current over the last 30,000 years. *Paleoceanography* 10, 763–773.
- Rasmussen, J.B.T., Polyak, V.J., Asmerom, Y., 2006. Evidence for Pacific-modulated precipitation variability during the late Holocene from the southwestern USA. *Geophys. Res. Lett.* 33, L08701. <http://dx.doi.org/10.1029/2006GL025714>.
- Rich, J., Stokes, S., 2011. A 200,000-year record of late Quaternary aeolian sedimentation on the Southern High Plains and nearby Pecos River Valley, USA. *Aeolian Res.* 2, 221–240. <http://dx.doi.org/10.1016/j.aeolia.2010.12.003>.
- Richey, J.N., Hollander, D.J., Flower, B.P., Eglington, T.I., 2011. Merging late Holocene molecular organic and foraminiferal-based geochemical records of sea surface temperature in the Gulf of Mexico. *Paleoceanography* 26, 1–12. <http://dx.doi.org/10.1029/2010PA002000>.
- Richey, J.N., Poore, R.Z., Flower, B.P., Quinn, T.M., 2007. 1400 yr multiproxy record of climate variability from the northern Gulf of Mexico. *Geology* 35, 423–426. <http://dx.doi.org/10.1130/G23507A.1>.
- Richey, J.N., Poore, R.Z., Flower, B.P., Quinn, T.M., Hollander, D.J., 2009. Regionally coherent little ice age cooling in the Atlantic warm pool. *Geophys. Res. Lett.* 36, 3–7. <http://dx.doi.org/10.1029/2009GL040445>.
- Scholz, D., Hoffmann, D.L., 2011. StalAge – an algorithm designed for construction of speleothem age models. *Quat. Geochronol.* 6, 369–382. <http://dx.doi.org/10.1016/j.quageo.2011.02.002>.
- Seager, R., Ting, M., Held, I., Kushnir, Y., Lu, J., Vecchi, G., Huang, H.-P., Harnik, N., Leetmaa, A., Lau, N.-C., Li, C., Velez, J., Naik, N., 2007. Model projections of an imminent transition to a more arid climate in southwestern North America. *Science* 316, 1181–1184. <http://dx.doi.org/10.1126/science.1139601>.
- Seager, R., Naik, N., Ting, M., Cane, M.A., Harnik, N., Kushnir, Y., 2010. Adjustment of the atmospheric circulation to tropical Pacific SST anomalies: Variability of transient eddy propagation in the Pacific-North America sector. *Q. J. R. Meteorol. Soc.* 136, 277–296. <http://dx.doi.org/10.1002/qj.588>.
- Sinclair, D.J., Banner, J.L., Taylor, F.W., Partin, J., Jenson, J., Mylroie, J., Goddard, E., Quinn, T.J., Jocson, J., Miklavčič, B., 2012. Magnesium and strontium systematics in tropical speleothems from the Western Pacific. *Chem. Geol.* 294–295, 1–17. <http://dx.doi.org/10.1016/j.chemgeo.2011.10.008>.
- Small, T.A., Hanson, J.A., 1994. *Geologic Framework and Hydrogeologic Characteristics of the Edwards Aquifer Outcrop, Comal County, Texas*. US Geol. Survey Water Res. Invest. Rep. 94–4117.
- Spotl, C., Fairchild, I.J., Toth, A.F., 2005. Cave air control on dripwater geochemistry, Obir Caves (Austria): Implications for speleothem deposition in dynamically ventilated caves. *Geochim. Cosmochim. Acta* 69, 2451–2468. <http://dx.doi.org/10.1016/j.gca.2004.12.009>.
- Thornalley, D.J.R., Elderfield, H., McCave, I.N., 2009. Holocene oscillations in temperature and salinity of the surface subpolar North Atlantic. *Nature* 457, 711–714. <http://dx.doi.org/10.1038/nature07717>.
- Timmermann, A., Okumura, Y., An, S.-I., Clement, A., Dong, B., Guiyadi, E., Hu, A., Jungclaus, J.H., Renold, M., Stocker, T.F., Stouffer, R.J., Sutton, R., Xie, S.-P., Yin, J., 2007. The influence of a weakening of the Atlantic meridional overturning circulation on ENSO. *J. Clim.* 20, 4899–4919. <http://dx.doi.org/10.1175/JCLI4283.1>.
- Toomey, R.S., Blum, M.D., Valastro, S., 1993. Late Quaternary climates and environments of the Edwards Plateau, Texas. *Glob. Planet. Change* 7, 299–320. [http://dx.doi.org/10.1016/0921-8181\(93\)90003-7](http://dx.doi.org/10.1016/0921-8181(93)90003-7).
- Toomey, R.S., 1993. *Late Pleistocene and Holocene Faunal and Environmental Changes at Hall's Cave, Kerr County, Texas*. Dissertation. The University of Texas at Austin.
- Tremaine, D.M., Froelich, P.N., 2013. Speleothem trace element signatures: a hydrologic geochemical study of modern cave dripwaters and farmed calcite. *Geochim. Cosmochim. Acta* 121, 522–545. <http://dx.doi.org/10.1016/j.gca.2013.07.026>.
- Troiani, B.T., Simms, A.R., Dellapenna, T., Piper, E., Yokoyama, Y., 2011. The importance of sea-level and climate change, including changing wind energy, on the evolution of a coastal estuary: copano Bay, Texas. *Mar. Geol.* 280, 1–19. <http://dx.doi.org/10.1016/j.margeo.2010.10.003>.
- USA Today, 2014. 10 states with the Fastest Growing Economies, 24/7 Wall St. <http://www.usatoday.com/story/money/business/2014/06/14/states-fastest-growing-economies-new/10377735>.
- van der Ent, R.J., Savenije, H.H.G., 2013. Oceanic sources of continental precipitation and the correlation with sea surface temperature. *Water Resour. Res.* 49, 3993–4004. <http://dx.doi.org/10.1029/wrcr.20296>.
- Vellinga, M., Wood, R.A., 2002. Global climate impacts of a collapse of the atlantic thermohaline circulation. *Clim. Chang.* 54, 251–267.

- Wagner, J.D.M., Cole, J.E., Beck, J.W., Patchett, P.J., Henderson, G.M., Barnett, H.R., 2010. Moisture variability in the southwestern United States linked to abrupt glacial climate change. *Nat. Geosci.* 3, 110–113. <http://dx.doi.org/10.1038/ngeo707>.
- Waters, M.R., Nordt, L.C., 1995. Late Quaternary floodplain history of the Brazos River in east-central Texas. *Quat. Res.* 43, 311–319. <http://dx.doi.org/10.1006/qres.1995.1037>.
- Weight, R.W.R., Anderson, J.B., Fernandez, R., 2011. Rapid mud accumulation on the central Texas shelf linked to climate change and sea-level rise. *J. Sed. Res.* 81, 743–764. <http://dx.doi.org/10.2110/jsr.2011.57>.
- Wilkins, D.E., Currey, D.R., 1999. Radiocarbon chronology and $d^{13}C$ analysis of mid-to late-Holocene aeolian environments, Guadalupe Mountains National Park, Texas, USA. *Holocene* 9, 363–371. <http://dx.doi.org/10.1191/09596399677728249>.
- Wong, C., Banner, J.L., 2010. Response of cave air CO₂ and drip water to brush clearing in central Texas: Implications for recharge and soil CO₂ dynamics. *J. Geophys. Res.* 115 <http://dx.doi.org/10.1029/2010JG001301>.
- Wong, C.I., Banner, J.L., Musgrove, M., 2011. Seasonal dripwater Mg/Ca and Sr/Ca variations driven by cave ventilation: Implications for and modeling of speleothem paleoclimate records. *Geochim. Cosmochim. Acta* 75, 3514–3529. <http://dx.doi.org/10.1016/j.gca.2011.03.025>.
- Wu, L., Li, C., Yang, C., Xie, S.P., 2008. Global teleconnections in response to a shutdown of the Atlantic meridional overturning circulation. *J. Clim.* 21, 3002–3019. <http://dx.doi.org/10.1175/2007JCLI1858.1>.
- Yamamoto, M., Yamamoto, M., Tanaka, Y., 2007. The California current system during the last 136,000 years: response of the North Pacific High to precessional forcing. *Quat. Sci. Rev.* 26, 405–414. <http://dx.doi.org/10.1016/j.quascirev.2006.07.014>.